European Journal of Haematology 84 (229–238)

ORIGINAL ARTICLE

BCR-ABL-independent and RAS/MAPK pathway-dependent form of imatinib resistance in Ph-positive acute lymphoblastic leukemia cell line with activation of EphB4

Momoko Suzuki[1,2], Akihiro Abe[1], Shizuka Imagama[3], Yuka Nomura[1], Ryohei Tanizaki[1], Yosuke Minami[1], Fumihiko Hayakawa[1], Yoshie Ito[4], Akira Katsumi[1], Kazuhito Yamamoto[5], Nobuhiko Emi[6], Hitoshi Kiyoi[7], Tomoki Naoe[1]

[1]Department of Hematology and Oncology, Nagoya University Graduate School of Medicine, Nagoya; [2]Department of Hematology, Komaki Municipal Hospital, Komaki, Aichi; [3]Department of Hematology, Nagoya Medical Center, Nagoya; [4]Yokkaichi City Public Health Center, Yokkaichi, Mie; [5]Department of Hematology, Aichi Cancer Center, Nagoya; [6]Department of Hematology, Fujita Health University, Toyoake, Aichi; [7]Department of Infectious Disease, Nagoya University Graduate School of Medicine, Nagoya, Japan

Abstract

Objective: We investigated the mechanism responsible for imatinib (IM) resistance in Philadelphia chromosome-positive acute lymphoblastic leukemia (Ph^+ ALL) cell lines. *Methods:* We established cell lines from a patient with Ph^+ ALL at the time of first diagnosis and relapsed phase and designated as NPhA1 and NPhA2, respectively. We also derived IM-resistant cells, NPhA2/STIR, from NPhA2 under gradually increasing IM concentrations. *Results:* NPhA1 was sensitive to IM (IC_{50} 0.05 μm) and NPhA2 showed mild IM resistance (IC_{50} 0.3 μm). NPhA2/STIR could be maintained in the presence of 10 μm IM. Phosphorylation of MEK and ERK was slightly elevated in NPhA2 and significantly elevated in NPhA2/STIR compared to NPhA1 cells. After treatment with IM, phosphorylation of MEK and ERK was not suppressed but rather increased in NPhA2 and NPhA2/STIR. Active RAS was also increased markedly in NPhA2/STIR after IM treatment. The expression of BCL-2 was increased in NPhA2 compared to NPhA1, but no further increase in NPhA2/STIR. Proliferation of NPhA2/STIR was significantly inhibited by a combination of MEK inhibitor and IM. Analysis of tyrosine phosphorylation status with a protein tyrosine kinase array showed increased phosphorylation of EphB4 in NPhA2/STIR after IM treatment. Although transcription of EphB4 was suppressed in NPhA1 and NPhA2 after IM treatment, it was not suppressed and its ligand, ephrinB2, was increased in NPhA2/STIR. Suppression of EphB4 transcripts by introducing short hairpin RNA into NPhA2/STIR partially restored their sensitivity to IM. *Conclusions:* These results suggest a new mechanism of IM resistance mediated by the activation of RAS/MAPK pathway and EphB4.

Key words Philadelphia chromosome-positive acute lymphoblastic leukemia; BCR-ABL; imatinib resistance; RAS/MAPK pathway; EphB4

Correspondence Akihiro Abe, MD, Department of Hematology and Oncology, Nagoya University Graduate School of Medicine, 65 Tsurumaicho, Showaku, Nagoya 466-8550, Japan. Tel: +81 52 744 2145; Fax: +81 52 744 2161; e-mail: aakihiro@med.nagoya-u.ac.jp

Accepted for publication 26 November 2009

doi:10.1111/j.1600-0609.2009.01387.x

The treatment of BCR-ABL-positive leukemia changed dramatically after the development of imatinib (IM). It has become a first-line agent in chronic phase chronic myelogenous leukemia (CML), and the 5-yr survival rate has improved greatly, together with a decrease in the rate of transformation to blastic crisis (1, 2). Acute lymphoblastic leukemia with Philadelphia chromosome (Ph^+ ALL) also arises from BCR-ABL positive progenitors, and use of IM in combination with conventional chemotherapy helps in extending the survival time (3). However, the effect of IM as a single agent for Ph^+ ALL is limited, and therefore relapse and resistance are continuing problems (4, 5).

Most prevalent mechanisms of IM resistance are point mutations in the kinase domain of ABL that preclude

the binding of IM (6, 7) and kinase inhibitors that overcome the effects of ABL kinase domain mutations have been developed (8). Many other mechanisms have also been reported to contribute to IM resistance; these include *BCR-ABL* gene amplification, BCR-ABL protein overexpression (9, 10), decreased intracellular IM concentration (11, 12), activation of other protein tyrosine kinases (PTKs) (13), and overexpression of BCL-2 (14). It has been reported that malignant hematopoietic progenitor cells from patients with CML are insensitive to IM and that CML stem cells remain in $CD34^+CD38^-$ fractions in bone marrow (BM) even after successful IM therapy (15, 16). Therefore, a strategy for overcoming BCR-ABL-independent IM resistance is an important requirement.

Although the mechanism of IM resistance in CML has been intensively investigated, fewer studies have examined IM resistance in Ph^+ ALL (17). Here, we investigated the mechanism of non-specifically induced mild resistance and IM-induced strong resistance in Ph^+ ALL cell lines.

Materials and methods

Patient and cell culture

The patient was a 64-yr-old woman who was diagnosed with Ph^+ ALL in 2002. She received chemotherapy and achieved remission, but relapsed 2 yr later. The karyotype was 46,XX,t(9;22)(q34;q11) at first diagnosis and relapsed phase. She had never been treated with IM. Heparinized BM samples were obtained with informed consent at initial diagnosis and during the relapse phase. Mononuclear cells were separated by Ficoll–Conray gradient centrifugation. The cells were cultivated in RPMI 1640 medium (Sigma, St. Louis, MO, USA) containing 20% fetal bovine serum (FBS) (Gibco-BRL, Grand Island, NY, USA), 100 IU/mL penicillin G (Meiji Seika, Tokyo, Japan), and 100 μg/mL streptomycin (Meiji Seika) and maintained in RPMI 1640 with 10% FBS. Cultures were performed at 37°C in a 5% CO_2-humidified atmosphere in an incubator. K562 cells were maintained in RPMI 1640 with 10% FBS.

Cell proliferation assay and reagents

To investigate the effect of kinase inhibitors on NPhA1, NPhA2, and NPhA2/STIR cells (2×10^4 per well) were added to 96-well plates in 100 μL RPMI containing 10% FBS with varying concentrations of IM, PI3-K inhibitor LY294002 (Promega, Madison, WI, USA), MEK inhibitor U0126 (Promega), SRC kinase inhibitor PP2 (Calbiochem, San Diego, CA, USA), or JAK2 inhibitor AG490 (Calbiochem). IM (Gleevec, STI-571) was provided by Novartis Pharmaceuticals (Basel, Switzerland). Tetra-Color One cell proliferation assay (Seikagaku Co., Tokyo, Japan) was performed as described previously (18). Briefly, the plates were incubated at 37°C for 72–96 h before the addition of a mixture of tetrazolium [2-(2-methoxy-4-nitrophenyl)-3-(4-nitrophenyl)-5-(2,4-disulfophenyl)-2H-tetrazolium, monosodium salt] and an electron carrier (1-methoxy-5-methylphenazium methylsulfate) (final volume 110 μL per well). The cells were incubated for an additional hour at 37°C, and absorption at 450 nm was measured using an ELISA plate reader.

Antibodies

The antibodies used were as follows: anti-phospho-AKT antiserum (Cell Signaling Technology, Beverly, MA, USA), rabbit anti-AKT antiserum (Cell Signaling Technology), rabbit anti-phospho-p44/42 MAPK antiserum (Cell Signaling Technology), rabbit anti-p44/42 MAPK antiserum (Cell Signaling Technology), rabbit anti-phospho-MEK 1/2 antiserum (Cell Signaling Technology), rabbit anti-MEK 1/2 antiserum (Cell Signaling Technology), rabbit anti-STAT3 antiserum (Santa Cruz Biotechnology, Santa Cruz, CA, USA), rabbit anti-phospho-STAT5 antiserum (Cell Signaling Technology), rabbit anti-STAT5A antiserum (R&D Systems, Minneapolis, MN, USA), rabbit anti-phospho-JAK2 antiserum (Upstate Biotechnology, Temecula, CA, USA), rabbit anti-JAK2 antiserum (Upstate Biotechnology), anti-phosphotyrosine mAb 4G10 (Millipore, Billerica, MA, USA), anti-EphB4 antiserum (R&D Systems), BCL2 (Cell Signaling Technology), BCL-X_L (Cell Signaling Technology), HRP-linked whole anti-mouse IgG antibody (GE Healthcare Bio-Sciences, Tokyo, Japan), and HRP-linked whole anti-mouse and anti-rabbit IgG antibody (GE Healthcare Bio-Sciences).

Flow cytometry

Cell surface antigens were determined by staining with a combination of phycoerythrin (PE)-conjugated antibodies and FITC-conjugated antibody, and analyzed by FACSCalibur (Becton Dickinson, Franklin Lakes, NJ, USA) according to the manufacturer's instructions. Samples were mixed and incubated with an appropriate volume of antibodies for 30 min on ice. The PE-conjugated antibodies used were anti-human CD13, CD33, CD56 antibodies (BD Biosciences, San Jose, CA, USA); anti-human CD2, CD5, CD7, and CD8 antibodies (Beckman Coulter, San Jose, CA, USA); and anti-CD10 antibody (Dako Cytomation, Fort Collins, CO, USA). The FITC-conjugated antibodies used were anti-human HLA-DR antibody (BD Biosciences), and anti-CD3, CD4, CD19, CD34, and CD41 antibodies (Beckman Coulter). An additional

reaction with FITC and PE-labeled isotype control antibodies (BD Biosciences) was performed as a negative control. A PE-conjugated monoclonal antibody of a murine anti-human Pgp (BD Biosciences) was used to determine the expression of the *MDR1* gene product. Analyses were performed using CELLQUEST software (BD). For DNA histograms, cells were washed with phosphate-buffered saline (PBS) and re-suspended in PBS containing 0.2% Triton X-100 and 50 g/mL propidium iodide (Sigma). Then, the DNA histograms were quantified by flow cytometry as described previously (19).

Western blotting

Cells were washed in PBS at 4°C and solubilized in a lysis buffer: 10 mM Tris–HCl (pH 7.8), 150 mM NaCl, 1% NP-40, 1 mM EDTA, CompleteMini™ protease inhibitor cocktail (Roche, Mannheim, Germany), and phosphatase inhibitor cocktail 1 and 2 (Sigma). The cell lysates were centrifuged, and the supernatants were corrected. For immunoblotting, cell lysates were boiled with electrophoresis SDS sample buffer for 3 min, separated by SDS/PAGE, and transferred onto polyvinylidine difluoride (PVDF) membranes (Bio-Rad, Hercules, CA, USA). The membrane blots were blocked with 5% skim milk in Tris–buffered saline (TBS) containing 0.1% Tween 20 (TBS-T) or with blocking buffer (15 mmol/L NaCl; 10 mmol/M malic acid; and 1% blocking reagent, pH 7.5, for the detection of 4G10) for 1 h at 37°C followed by incubation with primary antibodies in TBS-T for 2 h at room temperature. Following washing, the membranes were incubated with HRP-linked whole anti-mouse IgG antibody (GE Healthcare Bio-Sciences) in TBS-T for 2 h at room temperature. After washing, an enhanced chemiluminescence assay was performed and positive bands were detected on X-ray films.

RAS activation assay

pGEX-Raf-Ras binding domain (RBD) was a generous gift from Drs. Michinari Hamaguchi and Takashi Senga, Nagoya University. GST-Raf-RBD was purified and RAS activation was measured as described previously (20). In brief, the cells were treated with or without 10 μM IM for 4 h and then lysed with lysis buffer containing 25 mM Tris–HCl (pH 7.2), 150 mM NaCl, 1% NP-40, 1 mM dithiothreitol, 5 mM $MgCl_2$, 5% glycerol, 1 mM phenylmethylsulfonyl fluoride, and 10 μg/mL of aprotinin and 10 μg/mL of leupeptin at 4°C. The cell lysates were then centrifuged and supernatants were transferred to chilled Eppendorf tubes containing 20 μg of GST-Raf-RBD immobilized beads, and incubated for 1 h at 4°C. Small amounts (20 μL) of lysates were used as the loading control. The samples were washed four times with 1 mL lysis buffer, and eluted with 2× SDS loading buffer with 2% 2-mercaptoethanol. The samples were separated by 13% SDS-PAGE and transferred to PVDF membrane and then the immunoprecipitates were probed with anti-RAS antibody (Upstate Biotechnology).

Phosphorylation of tyrosine kinase protein array

Expression of phosphorylated PTKs was detected using the Phosphorylation Antibody Array kit (RayBiotech, Norcross, GA, USA). NPhA1, NPhA2, NPhA2/STIR, and IM-treated cells of these lines were washed and solubilized in cold cell lysis buffer. Samples were centrifuged, and supernatants were collected. One hundred micrograms of each sample was incubated with PTK array membranes spotted with various anti-PTK antibodies. Procedures were according to the manufacturer's protocol. Array signals were visualized by chemiluminescence detection using X-ray film. Densitometric quantifications of spot intensity were performed using an LAS-4000 mini image analyzer (Fujifilm, Tokyo, Japan).

Detection of EphB4 and ephrinB2 mRNA by reverse transcription (RT)-PCR

Total RNA was extracted from each cell line using RNA STAT-60™ (Tel-Test, Inc. Friendswood, TX, USA). First-strand cDNA was reverse-transcribed using oligo(dT) primers and moloney murine leukemia virus reverse transcriptase. PCR amplification was performed with TaKaRa Taq™ (Takara, Otsu, Japan) for 26 or 30 cycles using oligonucleotide primers (95°C for 30 s, 60°C for 30 s, 72°C for 1 min). The *EphB4* primers used were EphB4-1554F (5′-CGGCCAGGAACATCACAGCCAGAC-3′) and EphB4-1848R (5′-CACCTGCACCAATCACCTCTTCAATC-3′). The *ephrinB2* primers are ephrinB2-288F (5′-CCCTCTCCTCAACTGTGCCAAACC-3′) and ephrinB2-727R (5′-CAGCAAGAGGACCACCAGCGTGAT-3′). PCR reaction products were electrophoresed on 1.5% agarose gels and stained with ethidium bromide. Densitometric quantification of band intensity was analyzed as described earlier.

Induction of short hairpin (sh)RNA

Oligonucleotides for shRNA were designed and provided from iGENE Therapeutics (Tokyo, Japan). The oligonucleotides for EphB4-sh1 were sense (5′-GATCCGGGCAAATACGGATAGTATACGTGTGCTGTCCGTATACTGTCCGTGTTTGTCCTTTTTAT-3′) and antisense (5′-CGATAAAAAGGACAAACACGGACAGTATACGGACAGCACACGTATACTATCCGTATTTGCCCG-3′).

The oligonucleotides for EphB4-sh2 were sense (5′-GATCCGAGGGGACTTGTTTCGCTAACGTGTGCTGTCCGTTAGTGAAACAGGTTCCCTCTTTTTAT-3′) and antisense (5′-CGATAAAAAGAGGGAACCTGTTTCACTAACGGACAGCACACGTTAGCGAAACAAGTCCCCTCG-3′).

To construct shRNA-expressing retrovirus vectors, each set of primers was annealed and inserted between *Bam*HI and *Cla*I sites of the pSINsi-hU6 retroviral vector (Takara). Control vector carrying scramble oligonucleotide (pSINsi-hU6-SO) was purchased from Takara. To generate pseudotype viruses, we co-transfected 10 μg of pSINsi-hU6-SO, pSINsi-hU6/EphB4-sh1 or pSINsi-hU6/EphB4-sh2 with 10 μg pCGCGP using calcium phosphate co-precipitation, as reported previously (21). Culture medium was replaced with 8 mL fresh medium 8 h after transfection, and pseudotype virus was collected 48 h after transfection. To establish NPhA2/STIR/sh1 and NPhA2/STIR/sh2 cells, NPhA2/STIR cells were infected with 4 mL of each virus supernatant in the presence of 5 μg/mL protamine. After 48 h, the shRNA-expressing cells were selected with 1 mg/mL G418 (Sigma) in RPMI medium, and at 3 wk, the surviving cells were analyzed.

Results

Establishment of Ph$^+$ ALL cell lines and IM-resistant cell line

Continuously growing cells were obtained from BM samples at first diagnosis and in the relapse phase and were named NPhA1 and NPhA2, respectively; doubling times were 36 and 30 h, respectively. We cultured NPhA1 and NPhA2 cells with increasing concentrations of IM to generate IM-resistant sublines. The concentration of IM was initially 1 nM and increased gradually to 10 μM. Highly IM-resistant cells, named NPhA2/STIR cells, were obtained from NPhA2 after 6 months and maintained in the presence of 10 μM IM. Under this condition, the doubling time of the NPhA2/STIR line was about 36 h. IM-resistant cells could not be established from NPhA1. NPhA1 and NPhA2 were maintained over 1 yr and NPhA2/STIR was maintained over 6 months in the presence of 10 μM of IM before starting this study. These cell lines carry minor BCR-ABL and showed similar surface antigen expression: CD2$^-$, CD3$^-$, CD4$^-$, CD5$^-$, CD8$^-$, CD10$^+$, CD13^{low}, CD19$^+$, CD33$^-$, CD34$^-$, CD41$^-$, CD56$^-$. The karyotypes of NPhA1, NPhA2 and NPhA2/STIR in the metaphase cells were 45,XX, der(8;12)(q10;q10),t(9;22)(q34;q11)(6/6), 46,XX,t(9;22)(q34;q11)(18/18), and 46,XX, add(2)(q33),t(9;22)(q34;q11)(20/20), respectively. NPhA1 with additional chromosomal abnormality was clonally selected from the primitive leukemia cells at first diagnosis, but NPhA2 has the same abnormality with the primitive leukemia cells at relapse phase. NPhA2/STIR obtained additional chromosomal abnormality of add(2)(q33) to NPhA2, which may relate with IM resistance.

Characterization of IM resistance in NPhA2 and NPhA2/STIR cells

Tetra Color One cell proliferation assays were performed on cells exposed to 0.01, 0.03, 0.1, 0.3, 1, 3, or 10 μM IM

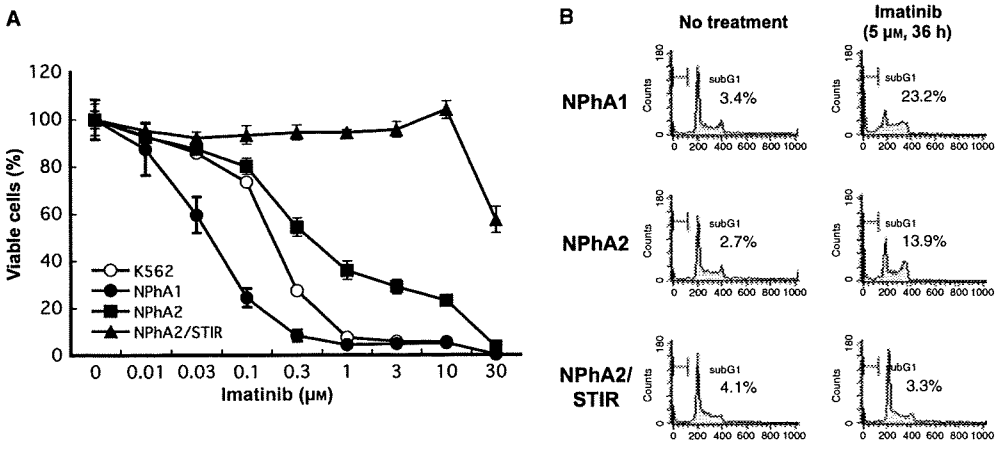

Figure 1 Characterization of imatinib (IM) sensitivity of NPhA1, NPhA2, and NPhA2/STIR cells. (A) IM sensitivity of cell lines derived from a Philadelphia chromosome-positive acute lymphoblastic leukemia patient. Each cell line was incubated with IM at the indicated concentration for 96 h. The cell proliferation assay was performed in triplicate, and mean absorption values with standard deviations are represented. Three repeat experiments showed similar results. (B) Cell cycle analysis by propidium iodide staining after treatment with IM. Each cell line was cultured in the presence or absence of 5 μM IM for 36 h. The cell cycle and cell death were evaluated by FACS analysis.

(Fig. 1A). On day 4, we evaluated the concentration of IM necessary to induce a 50% decrease in the number of viable cells as measured by the OD index. The IC_{50} was 0.05 μM for NPhA1, 0.3 μM for NPhA2, and 30 μM for NPhA2/STIR. NPhA2 cells acquired non-specifically induced IM resistance after a series of conventional chemotherapy without IM. NPhA1 cells were more sensitive but NPhA2 cells were more resistant to IM than K562 cells. Moreover, the concentration of IM needed for 50% reduction in the number of viable cells after 4 d of exposure to IM was about 100 times higher in the resistant NPhA2/STIR line compared to that in NPhA2 cells. Lines NPhA1 and NPhA2 did not show cell cycle-specific arrest, but the subG1 fraction increased after treatment with IM (Fig. 1B). IM did not affect the cell cycle distribution in NPhA2/STIR cells. Surface expression of MDR1 was not detected in NPhA2 and NPhA2/STIR cells by FACS analysis. No mutation was detected by direct sequencing with RT-PCR in kinase domain of the *BCR-ABL* gene (data not shown).

Phosphorylation of molecules involved in cell proliferation after IM treatment

We examined the phosphorylation of molecules that are involved in cell proliferation after IM treatment (Fig. 2A). Each cell was treated with IM for 6 h, and cell lysates were subjected to western blot analysis. The phosphorylation of BCR-ABL was decreased in NPhA2 cells, and phosphorylation of STAT5 paralleled with that of phospho-BCR-ABL after IM treatment. The phosphorylation level of MEK, ERK, and STAT3 was higher in NPhA2 compared with NPhA1 cells and was higher in NPhA2/STIR cells than in NPhA2 and NPhA1 cells. In particular, although phosphorylation of ABL was completely absent in all cells and phosphorylation of STAT5 was also suppressed, phosphorylation of MEK and ERK was increased in NPhA2, and especially in NPhA2/STIR cells, when treated with 10 μM IM for 6 h. Phosphorylation of AKT did not show any difference after IM treatment. We also examined expression of BCL-2 and BCL-X_L, and found that BCL-2 was increased but BCL-X_L was not altered in NPhA2 and NPhA2/STIR cells.

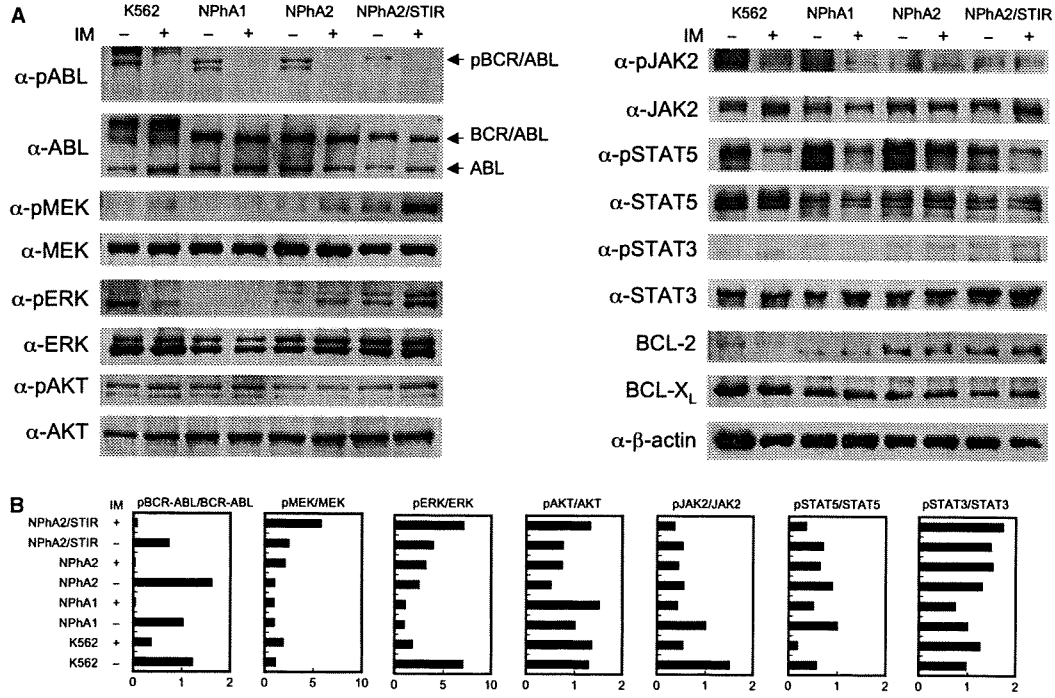

Figure 2 Phosphorylation and expression of molecules involved in cell proliferation and survival after imatinib (IM) treatment. (A) Phosphorylation and expression of signal molecules were analyzed by western blotting. Each cell line was treated or not treated with 10 μM IM for 6 h. Phosphorylation of ABL, MEK, ERK, AKT, JAK2, STAT5, and STAT3 was detected by phosphospecific antibodies. Expression of BCL-2 and BCL-X_L proteins is also shown. The experiments were repeated three times and showed similar results. (B) For quantification of band intensities, western blots were scanned with a high-resolution scanner, and the density of bands was quantified using IMAGEJ software (NIH, Bethesda, MD, USA). The data were shown as phosphorylated to total protein ratio that was calculated as relative value to the data of NPhA1 without IM as 1.

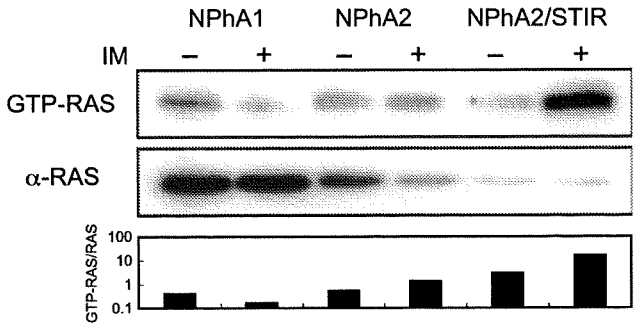

Figure 3 RAS activation assay. Each cell line was treated or not treated with 10 μM imatinib for 4 h and then the RAS assay was performed. Band intensities were determined as described before and shown as the value of GTP-RAS to total RAS ratio.

MEK/ERK is a downstream signaling protein of the RAS pathway. Therefore, we next examined RAS activity after IM treatment. We found that RAS was activated in NPhA1, NPhA2, and NPhA2/STIR cells, and that active RAS was decreased in NPhA1, but significantly increased in NPhA2/STIR cells after 4 h of exposure to 10 μM IM, although the basic level of expression of RAS protein was decreased in NPhA2/STIR cells (Fig. 3). These results indicate that the enhanced activation of MEK–MAPK pathway by IM in NPhA2/STIR cells occurred downstream of RAS activation.

Sensitivity to kinase inhibitors

We analyzed the sensitivity of NPhA1, NPhA2, and NPhA2/STIR cells to the kinase inhibitors MEK inhibitor (U0126), PI3K inhibitor (LY249002), SRC family kinase inhibitor (PP2), and JAK2 inhibitor (AG490). As shown in Fig. 4A, U0126 partially inhibited cell proliferation, especially in NPhA2/STIR cells. LY249002 and AG490 partially inhibited proliferation, but there was no specificity for IM-resistant cells. PP2 did not have any significant effects.

Combined treatment with the MEK inhibitor and IM had a synergistic effect on the suppression of NPhA2 proliferation, but synergism was not observed when the PI3K inhibitor was combined with IM (Fig. 4B).

Analysis of phosphorylation of PTKs

Phosphorylation of PTKs may contribute to IM resistance. To explore this possibility, the phosphorylation level of PTKs was determined using the Phosphorylation

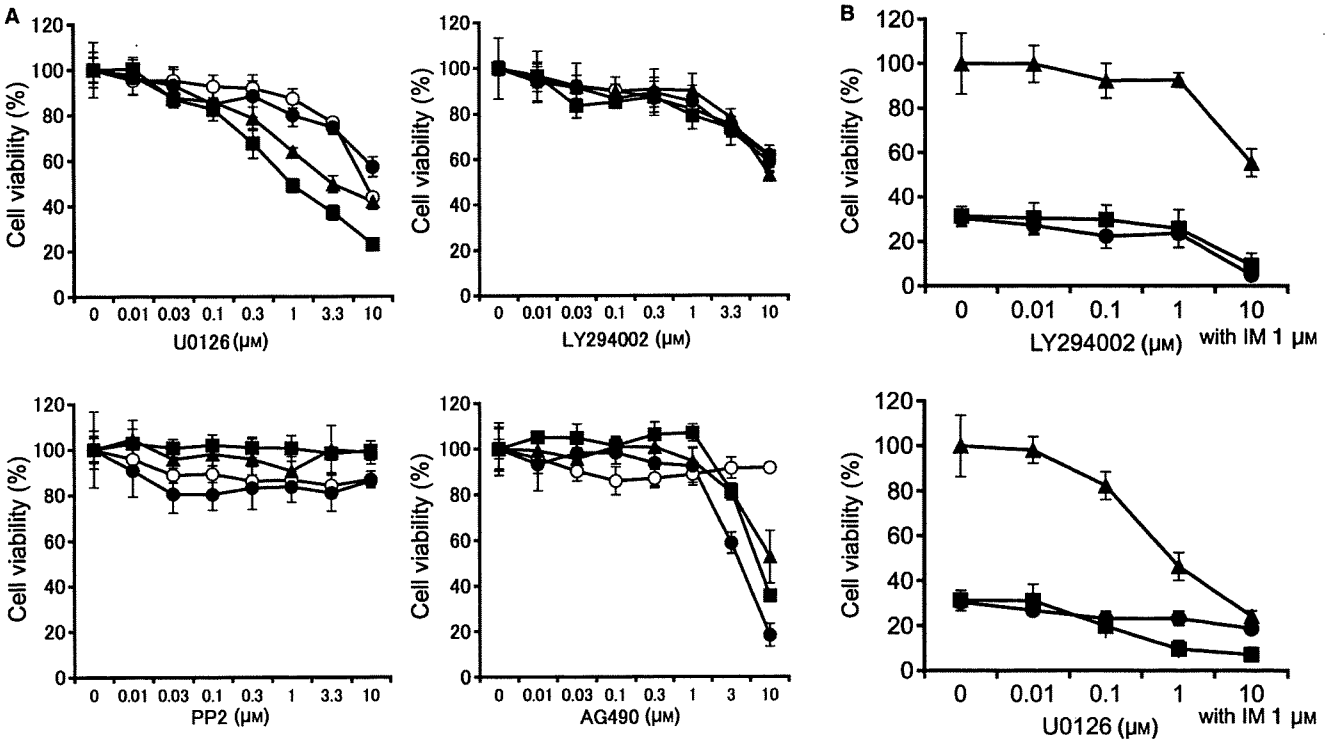

Figure 4 Sensitivity to kinase inhibitors and their combination. (A) Effect of MEK inhibitor (U0126), PI3K inhibitor (LY249002), SRC family kinase inhibitor (PP2), and JAK2 inhibitor (AG490) in K562 (○), NPhA1 (●), NPhA2 (■), and NPhA2/STIR (▲) cells was examined with the Tetra Color One assay. (B) Combined effect of imatinib (IM) with LY249002 or U0126. NPhA1 (●), NPhA2 (■), and NPhA2/STIR (▲) cells were incubated with 1 μM IM and LY249002 or U0126 at the indicated concentration for 96 h. The cell proliferation assay was performed in triplicate, and mean absorption values with standard deviations are represented.

Antibody Array kit with cell lysates of NPhA1, NPhA2, and NPhA2/STIR cells and corresponding IM-treated cells. This phospho-PTK array can simultaneously profile 71 different known human phosphorylated PTKs. The assay conserves time and samples because a large number of PTKs can be evaluated simultaneously using the same quantity of sample. Phosphorylation status was analyzed by densitometric quantification, and data for representative PTKs are shown in Fig. 5. The quality of the array was confirmed by the phosphorylation level of BCR-ABL, which was suppressed after the IM treatment and was consistent with the data of western blotting (Fig. 2). Phosphorylation of many Src family kinases, LYN, HCK and FGR, was suppressed after treatment with IM, and this suppression was paralleled by phosphorylation of BCR-ABL (Fig. 5). Phosphorylation of JAK2 was also inhibited by IM in three NPhA cell lines (Figs 2 and 5). Note that phosphorylation of EphB4 was increased in NPhA2/STIR cells after treatment with IM, but decreased in NPhA1 and NPhA2 cells. We therefore analyzed the role of EphB4 in the IM resistance of NPhA2/STIR cells.

Expression of EphB4 and ephrinB2 and phosphorylation of EphB4 in each cell line

We analyzed the mRNA expression of *EphB4* and *ephrinB2* in NPhA1, NPhA2, and NPhA2/STIR cells before and after treatment with IM (Fig. 6A). The expression of *EphB4* was inhibited in NPhA1 and NPhA2, but was not changed in NPhA2/STIR cells after treatment with IM. The expression of *ephrinB2* was increased in NPhA2 cells, which showed mild IM resistance, but the *EphB4* was inhibited after IM treatment. NPhA2/STIR cells showed higher expression of *EphB4* and *ephrinB2* than NPhA1 cells, with no decrease even after IM treatment. The phosphorylation of EphB4 was inhibited in NPhA1and NPhA2 cells but increased in NPhA2/STIR cells after treatment with IM (Fig. 6B).

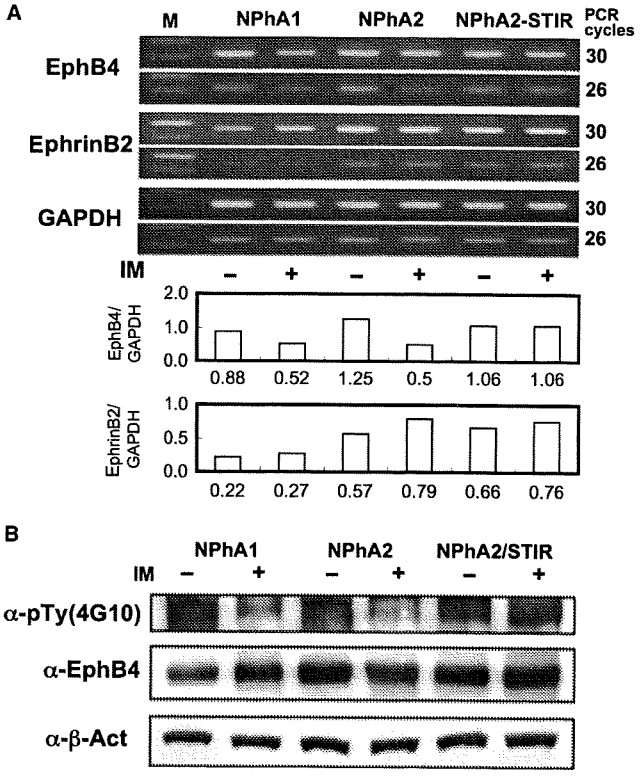

Figure 6 Expression of EphB4 and ephrinB2 and phosphorylation of EphB4. (A) Expression of *EphB4* and *ephrinB2* transcripts was compared by reverse transcription-PCR among NPhA1, NPhA2, and NPhA2/STIR cells before and after treatment with imatinib. Band intensity on gel electrophoresis was quantified using computer software as described in the text. (B) Expression and phosphorylation of EphB4 were analyzed by Western blotting. Whole-cell lysates were separated by SDS-PAGE, transferred to Hybond-C Extra membranes (GE Healthcare Bio-Sciences) and detected with the indicated antibodies.

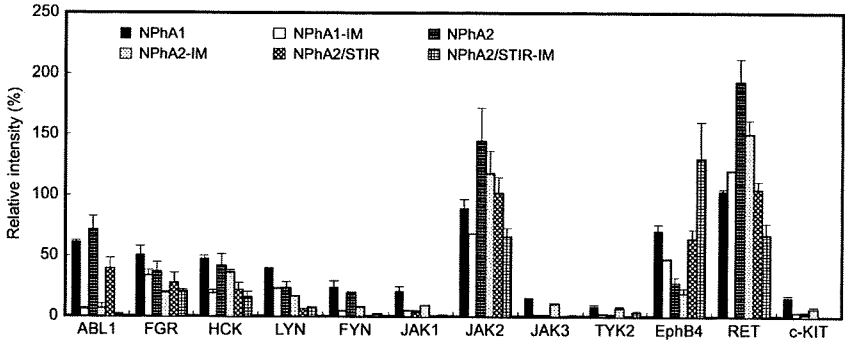

Figure 5 Phosphorylation antibody array analyses. Phosphorylated protein tyrosine kinases were detected using an antibody array. Imatinib-treated or untreated cell lysates were added to the antibody array membrane. Then, the membranes were washed and biotinylated anti-phosphotyrosine antibody was used to detect phosphorylated tyrosines on activated receptors. After incubation with HRP-conjugated streptavidin, array signals were visualized by chemiluminescent detection using X-ray film, and spot intensity was measured densitometrically.

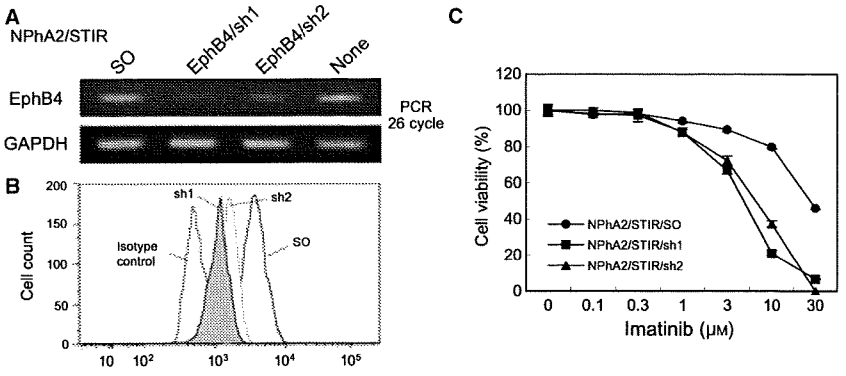

Figure 7 Analysis of EphB4 as a target of imatinib (IM) resistance. (A) Expression of *EphB4* transcript was inhibited with short hairpin (sh)RNA. We transduced the shRNAs sequence for *EphB4* or scramble oligonucleotide (SO) into NPhA2/STIR cells with a retroviral vector. Expression of *EphB4* transcript was analyzed by reverse transcription-PCR. (B) Surface expression of EphB4 was detected by FACS analysis. (C) Sensitivity of NPhA2/STIR/SO, NPhA2/STIR/sh1 and NPhA2/STIR/sh2 cells to IM. NPhA2/STIR/SO, NPhA2/STIR/sh1, and NPhA2/STIR/sh2 cells were added to 96-well plates with different concentrations of IM. Plates were incubated at 37°C for 96 h before addition of a mixture of tetrazolium and electron carrier. The cell proliferation assay was performed in triplicate, and mean absorption values are shown with their standard deviations. Three repeat experiments showed similar results.

Inhibition of EphB4 with shRNA

To analyze the role of EphB4 in IM resistance, EphB4 was knocked down with shRNA expressed by a retroviral vector. We tried two kinds of sh sequence, and established NPhA2/STIR/sh1 and NPhA2/STIR/sh2 cells in which the expression of *EphB4 RNA* was suppressed (Fig. 7A). FACS analysis showed that surface expression of EphB4 was reduced (Fig. 7B). The growth of NPhA2/STIR/sh1 and NPhA2/STIR/sh2 cells was inhibited by IM at concentrations above 3 μM; these cells were more sensitive than NPhA2/STIR but less sensitive than NPhA2 cells (Fig. 7C).

Discussion

We established cell lines derived from a patient with Ph^+ ALL and designated them NPhA1 (cells recovered at first diagnosis) and NPhA2 (cells recovered in the relapse phase). We also developed the IM-resistant cell line NPhA2/STIR from NPhA2 cells. NPhA2 cells showed mild IM resistance, and NPhA2/STIR proliferated in the presence of 10 μM IM, indicating strong IM resistance.

We examined the intracellular signaling pathway of these cell lines before and after IM treatment. NPhA2 cells acquired non-specific IM resistance in the relapse phase after conventional chemotherapy. Phosphorylation of LYN, HCK, FGR and JAK2, which were possible to be activated downstream of BCR-ABL (22, 23), was inhibited by IM, so that they were not likely to relate with IM-resistance in NPhA2 and NPhA2/STIR. Mild increases in MEK, ERK, and STAT3 phosphorylation and BCL-2 expression may be responsible for the mild IM resistance of NPhA2 cells. After IM treatment, NPhA2/STIR cells showed increased phosphorylation of MEK and ERK and a marked increase in RAS activation, which may play a role in BCR-ABL-independent strong IM resistance. Persistent activation of EphB4 after treatment with IM may be a partial contributor to the IM resistance of NPhA2/STIR cells.

The RAS signaling pathway plays an essential role in cancer cell growth. RAS activation leads to the phosphorylation and activation of downstream signaling proteins such as MEK and MAPK. Activation of the MAPK pathway was suggested as an explanation for the incomplete effect of IM on CML (24, 25). The RAS-independent activation of the MEK–MAPK pathway after IM administration was reported in pancreatic cancers, and addition of MEK inhibitor enhanced the inhibitory effect of IM on cancer cell growth (26). In our study, RAS was activated upstream of the MEK–MAPK pathway, but NRAS and KRAS mutations were not detected (data not shown). We obtained evidence that the induction of MEK–MAPK activation was induced after treatment with IM. IM may cancel negative feedback directed to the RAS–MAPK pathway or stimulate upstream RAS signaling. These results suggest a potential role for combined therapy with MEK inhibitor and IM in patients with BCR-ABL-independent IM resistance.

EphB4 is a member of the largest family of transmembrane receptor tyrosine kinases and has been shown to be related to the survival signal in several types of human malignant cells (27, 28), such as breast cancer, ovarian cancer, and squamous cell carcinoma cells. The significance of EphB4 and ephrinB2 coexpression in tumor advancement has also been described (29, 30). EphB4 is expressed in immature hematopoietic cells and its ligand ephrinB2 is expressed on BM stromal

cells and arterial endothelial cells (31). In this study, we screened 71 kinds of tyrosine kinase to determine their phosphorylation status using a tyrosine kinase antibody array and found that EphB4 was activated in Ph^+ cell lines. Activation of EphB4 was suppressed after IM treatment in NPhA1 and NPhA2 but not in NPhA2/STIR cells with increased expression of EphB4 and ephrinB2 transcripts. Although partial restoration of sensitivity to IM in NPhA2/STIR cells was observed after the introduction of EphB4 shRNA, the sensitivity of shRNA-containing NPhA2/STIR cells was not completely restored to the NPhA2 level. This may be a result of insufficient EphB4 suppression or the cumulative effects of other resistance mechanisms. The relationship between EphB4 and RAS activation remains to be elucidated in future studies.

We present here a new mechanism of IM resistance, i.e., the induction of RAS/MAPK activation, possibly related to EphB4. The results of this study also suggest a potential role of combined therapy with RAS/MAPK inhibitors and IM for Ph^+ ALL.

Acknowledgements

We thank Satoshi Suzuki and Chika Wakamatsu of Nagoya University for their skillful technical assistance. This study was supported by Grants-in-Aid from the Ministry of Education, Culture, Sports, Science and Technology, and the National Institute of Biomedical Innovation.

References

1. Druker BJ, Guilhot F, O'Brien SG, *et al.* Five-year follow-up of patients receiving imatinib for chronic myeloid leukemia. *N Engl J Med* 2006;**355**:2408–17.
2. O'Brien SG, Guilhot F, Larson RA, *et al.* Imatinib compared with interferon and low-dose cytarabine for newly diagnosed chronic-phase chronic myeloid leukemia. *N Engl J Med* 2003;**348**:994–1004.
3. Yanada M, Takeuchi J, Sugiura I, *et al.* High complete remission rate and promising outcome by combination of imatinib and chemotherapy for newly diagnosed BCR-ABL-positive acute lymphoblastic leukemia: a phase II study by the Japan Adult Leukemia Study Group. *J Clin Oncol* 2006;**24**:460–6.
4. Druker BJ, Sawyers CL, Kantarjian H, Resta DJ, Reese SF, Ford JM, Capdeville R, Talpaz M. Activity of a specific inhibitor of the BCR-ABL tyrosine kinase in the blast crisis of chronic myeloid leukemia and acute lymphoblastic leukemia with the Philadelphia chromosome. *N Engl J Med* 2001;**344**:1038–42.
5. Ottmann OG, Druker BJ, Sawyers CL, *et al.* A phase 2 study of imatinib in patients with relapsed or refractory Philadelphia chromosome-positive acute lymphoid leukemias. *Blood* 2002;**100**:1965–71.
6. Hofmann WK, Jones LC, Lemp NA, de Vos S, Gschaidmeier H, Hoelzer D, Ottmann OG, Koeffler HP. Ph(+) acute lymphoblastic leukemia resistant to the tyrosine kinase inhibitor STI571 has a unique BCR-ABL gene mutation. *Blood* 2002;**99**:1860–2.
7. Shah NP, Nicoll JM, Nagar B, Gorre ME, Paquette RL, Kuriyan J, Sawyers CL. Multiple BCR-ABL kinase domain mutations confer polyclonal resistance to the tyrosine kinase inhibitor imatinib (STI571) in chronic phase and blast crisis chronic myeloid leukemia. *Cancer Cell* 2002;**2**:117–25.
8. Redaelli S, Piazza R, Rostagno R, Magistroni V, Perini P, Marega M, Gambacorti-Passerini C, Boschelli F. Activity of bosutinib, dasatinib, and nilotinib against 18 imatinib-resistant BCR/ABL mutants. *J Clin Oncol* 2009;**27**:469–71.
9. le Coutre P, Tassi E, Varella-Garcia M, Barni R, Mologni L, Cabrita G, Marchesi E, Supino R, Gambacorti-Passerini C. Induction of resistance to the Abelson inhibitor STI571 in human leukemic cells through gene amplification. *Blood* 2000;**95**:1758–66.
10. Scappini B, Gatto S, Onida F, *et al.* Changes associated with the development of resistance to imatinib (STI571) in two leukemia cell lines expressing p210 Bcr/Abl protein. *Cancer* 2004;**100**:1459–71.
11. Mahon FX, Belloc F, Lagarde V, Chollet C, Moreau-Gaudry F, Reiffers J, Goldman JM, Melo JV. MDR1 gene overexpression confers resistance to imatinib mesylate in leukemia cell line models. *Blood* 2003;**101**:2368–73.
12. White DL, Saunders VA, Dang P, Engler J, Zannettino AC, Cambareri AC, Quinn SR, Manley PW, Hughes TP. OCT-1-mediated influx is a key determinant of the intracellular uptake of imatinib but not nilotinib (AMN107): reduced OCT-1 activity is the cause of low in vitro sensitivity to imatinib. *Blood* 2006;**108**:697–704.
13. Donato NJ, Wu JY, Stapley J, Gallick G, Lin H, Arlinghaus R, Talpaz M. BCR-ABL independence and LYN kinase overexpression in chronic myelogenous leukemia cells selected for resistance to STI571. *Blood* 2003;**101**:690–8.
14. Dai Y, Rahmani M, Corey SJ, Dent P, Grant S. A Bcr/Abl-independent, Lyn-dependent form of imatinib mesylate (STI-571) resistance is associated with altered expression of Bcl-2. *J Biol Chem* 2004;**279**:34227–39.
15. Abe A, Minami Y, Hayakawa F, *et al.* Retention but significant reduction of BCR-ABL transcript in hematopoietic stem cells in chronic myelogenous leukemia after imatinib therapy. *Int J Hematol* 2008;**88**:471–5.
16. Graham SM, Jorgensen HG, Allan E, Pearson C, Alcorn MJ, Richmond L, Holyoake TL. Primitive, quiescent, Philadelphia-positive stem cells from patients with chronic myeloid leukemia are insensitive to STI571 in vitro. *Blood* 2002;**99**:319–25.
17. Mishra S, Zhang B, Cunnick JM, Heisterkamp N, Groffen J. Resistance to imatinib of bcr/abl p190 lymphoblastic leukemia cells. *Cancer Res* 2006;**66**:5387–93.
18. Abe A, Kiyoi H, Ninomiya M, *et al.* Establishment of a stroma-dependent human acute myelomonocytic leukemia

cell line, NAMO-2, with FLT3 tandem duplication. *Int J Hematol* 2006;**84**:328–36.
19. Minami Y, Yamamoto K, Kiyoi H, Ueda R, Saito H, Naoe T. Different antiapoptotic pathways between wild-type and mutated FLT3: insights into therapeutic targets in leukemia. *Blood* 2003;**102**:2969–75.
20. Taylor SJ, Resnick RJ, Shalloway D. Nonradioactive determination of Ras-GTP levels using activated ras interaction assay. *Methods Enzymol* 2001;**333**:333–42.
21. Abe A, Emi N, Kanie T, Imagama S, Kuno Y, Takahashi M, Saito H, Naoe T. Expression cloning of oligomerization-activated genes with cell-proliferating potency by pseudotype retrovirus vector. *Biochem Biophys Res Commun* 2004;**320**:920–6.
22. Hu Y, Liu Y, Pelletier S, Buchdunger E, Warmuth M, Fabbro D, Hallek M, Van Etten RA, Li S. Requirement of Src kinases Lyn, Hck and Fgr for BCR-ABL1-induced B-lymphoblastic leukemia but not chronic myeloid leukemia. *Nat Genet* 2004;**36**:453–61.
23. Xie S, Wang Y, Liu J, Sun T, Wilson MB, Smithgall TE, Arlinghaus RB. Involvement of Jak2 tyrosine phosphorylation in Bcr-Abl transformation. *Oncogene* 2001;**20**:6188–95.
24. Agarwal A, Eide CA, Harlow A, Corbin AS, Mauro MJ, Druker BJ, Corless CL, Heinrich MC, Deininger MW. An activating KRAS mutation in imatinib-resistant chronic myeloid leukemia. *Leukemia* 2008;**22**:2269–72.
25. Chu S, Holtz M, Gupta M, Bhatia R. BCR/ABL kinase inhibition by imatinib mesylate enhances MAP kinase activity in chronic myelogenous leukemia CD34+ cells. *Blood* 2004;**103**:3167–74.
26. Takayama Y, Kokuryo T, Yokoyama Y, Nagino M, Nimura Y, Senga T, Hamaguchi M. MEK inhibitor enhances the inhibitory effect of imatinib on pancreatic cancer cell growth. *Cancer Lett* 2008;**264**:241–9.
27. Kumar SR, Singh J, Xia G, *et al.* Receptor tyrosine kinase EphB4 is a survival factor in breast cancer. *Am J Pathol* 2006;**169**:279–93.
28. Scehnet JS, Ley EJ, Krasnoperov V, Liu R, Manchanda PK, Sjoberg E, Kostecke AP, Gupta S, Kumar SR, Gill PS. The role of Ephs, Ephrins and growth factors in Kaposi sarcoma and implications of EphrinB2 blockade. *Blood* 2008;**113**:254–63.
29. Alam SM, Fujimoto J, Jahan I, Sato E, Tamaya T. Coexpression of EphB4 and ephrinB2 in tumour advancement of ovarian cancers. *Br J Cancer* 2008;**98**:845–51.
30. Yavrouian EJ, Sinha UK, Rice DH, Salam MT, Gill PS, Masood R. The significance of EphB4 and EphrinB2 expression and survival in head and neck squamous cell carcinoma. *Arch Otolaryngol Head Neck Surg* 2008;**134**:985–91.
31. Suenobu S, Takakura N, Inada T, Yamada Y, Yuasa H, Zhang XQ, Sakano S, Oike Y, Suda T. A role of EphB4 receptor and its ligand, ephrin-B2, in erythropoiesis. *Biochem Biophys Res Commun* 2002;**293**:1124–31.

Bone Marrow Transplantation (2010) 45, 363–369

www.nature.com/bmt

ORIGINAL ARTICLE

Donor single nucleotide polymorphism in the *CCR9* gene affects the incidence of skin GVHD

Y Inamoto[1,2], M Murata[1], A Katsumi[1], Y Kuwatsuka[2], A Tsujimura[2], Y Ishikawa[1], K Sugimoto[1], M Onizuka[2], S Terakura[1], T Nishida[2], T Kanie[2], H Taji[2], H Iida[2], R Suzuki[2], A Abe[1], H Kiyoi[3], T Matsushita[1], K Miyamura[2], Y Kodera[2] and T Naoe[1]

[1]*Department of Hematology and Oncology, Nagoya University Graduate School of Medicine, Nagoya, Japan;* [2]*Department of Hematology, Japanese Red Cross Nagoya First Hospital, Nagoya, Japan and* [3]*Department of Infectious Diseases, Nagoya University Graduate School of Medicine, Nagoya, Japan*

The interactions between chemokines and their receptors may have an important role in initiating GVHD after allogeneic hematopoietic SCT (allo-HSCT). CCL25 and CCR9 are unique because they are exclusively expressed in epithelial cells and in Peyer's patches of the small intestine. We focused on rs12721497 (G926A), one of the non-synonymous single nucleotide polymorphisms (SNPs) in the *CCR9* gene, and analyzed the SNP of donors in 167 consecutive patients who received allo-HSCT from an HLA-identical sibling donor. Genotypes were tested for associations with acute and chronic GVHD in each organ and transplant outcome. Multivariate analyses showed that the genotype 926AG was significantly associated with the incidence of acute stage ⩾2 skin GVHD (hazard ratio: 3.2; 95% confidence interval (95% CI): 1.1–9.1; $P=0.032$) and chronic skin GVHD (hazard ratio: 4.1; 95% CI: 1.1–15; $P=0.036$), but not with GVHD in other organs or with relapse, non-relapse mortality or OS. To clarify the functional differences between genotypes, each SNP in retroviral vectors was transfected into Jurkat cells. In chemotaxis assays, the 926G transfectant showed greater response to CCL25 than the 926A transfectant. In conclusion, more active homing of *CCR9*-926AG T cells to Peyer's patches may produce changes in Ag presentation and result in increased incidence of skin GVHD.
Bone Marrow Transplantation (2010) **45,** 363–369; doi:10.1038/bmt.2009.131; published online 15 June 2009
Keywords: allogeneic transplantation; CCR9; chemokine; gene polymorphism; GVHD

Correspondence: Dr A Katsumi, Department of Hematology and Oncology, Nagoya University Graduate School of Medicine, 65 Tsurumai-cho, Showa-ku, Nagoya 466-8560, Japan.
E-mail: katsumi@med.nagoya-u.ac.jp
Received 3 February 2009; revised 22 April 2009; accepted 24 April 2009; published online 15 June 2009

Introduction

Acute GVHD is a severe complication of allogeneic hematopoietic SCT (allo-HSCT).[1] After Ag presentation in secondary lymphoid tissues, migration of activated donor T lymphocytes to target organs has a central role in its induction. Recent studies have shown that the migration of lymphocytes to secondary lymphoid tissues or target organs, such as the skin, liver and gut, is regulated by specific chemokines.[2,3] Chemokines are a group of small molecules that regulate the trafficking of leukocytes through interactions with a subset of seven transmembrane, G protein-coupled receptors (chemokine receptors).[4,5] Their interactions may have an important role in initiating organ-specific GVHD.

Sites of expression are ubiquitous in many chemokines. For example, CCL17, which is well known as a skin-homing chemokine, is also expressed in many other organs, including the adrenal gland, bronchus, cerebellum, colon, heart and liver.[4] CCL28 is expressed by epithelial cells in several mucosal tissues, including the trachea, small intestine, colon, rectum, salivary gland and mammary gland.[6,7] By contrast, CCL25 (thymus-expressed chemokine) and its receptor CCR9 are unique because, outside the thymus, they are almost exclusively expressed by epithelial cells and Peyer's patches in the small intestine.[8–10] Therefore, we focused on CCR9 because it may influence the onset of intestinal GVHD or Ag presentation in Peyer's patches.

The *CCR9* gene is located on chromosome 3p21.3. A variety of single nucleotide polymorphisms (SNPs) in the *CCR9* gene have been reported, although their functional differences are not yet known. Within these SNPs, rs12721497 (G926A) is non-synonymous in exons, and it is the sole SNP whose frequency and linkage disequilibrium have been reported. This SNP alters the CCR9 amino acid sequence of the third exoloop from Val272 to Met272. We hypothesize that this SNP may have an effect on the onset of GVHD and transplant outcome because of the differences in the tissue-specific migration of T lymphocytes.

Materials and methods

Patients

A total of 186 consecutive patients received allogeneic BM or PBSC transplantation from an HLA-identical sibling donor at the Nagoya University Hospital and the Japanese Red Cross Nagoya First Hospital between 1987 and 2006. HLA matching among donor–recipient pairs was confirmed by either family study or genotyping in all patients. Of these 186 patients, 167 who received T-cell-replete transplantation and CYA in combination with short-term MTX as a GVHD prophylaxis were selected to participate in the study. CYA was administered daily at 3.0 mg/kg from day 1 as an i.v. infusion, and then switched to an oral dose at twice the i.v. dose when oral intake resumed. MTX was administered at 10 mg/m^2 on day 1 and, on days 3 and 6, was administered at 7 mg/m^2. Informed consent was obtained from all patients and donors, and the study was approved by the ethics committees at the Nagoya University Hospital and Japanese Red Cross Nagoya First Hospital.

Allellic discrimination of the polymorphism G926A in the CCR9 gene

The *CCR9*-G926A polymorphism (rs12721497) was determined by the PCR-RFLP method using genomic DNA obtained from donor PBMCs. The primers used for PCR were 5′-CACACCCTGATACAAGCCAA (forward) and 5′-CTCCAGCAACATAGACGACA (reverse). Sequences of interest were amplified by PCR, using Advantage II Polymerase Mix (Clontech Laboratories, Mountain View, CA, USA) in reaction mixtures containing 0.5 μl of genomic DNA and 10 pmol of each primer in a volume of 20 μl. Amplifications were performed using 35 cycles of denaturation at 95 °C for 30 s, annealing at 65 °C for 15 s and elongation at 72 °C for 30 s on a model 9600 thermocycler (Perkin-Elmer, Norwalk, CT, USA). After amplification, the 369-bp *CCR9* fragment was digested for 2 h at 37 °C with 5 U of *NLA*III (New England BioLabs, Ipswich, MA, USA) in a 20 μl reaction mixture. The digested products were analyzed by electrophoresis on a 1.5% agarose gel. Wild-type (AA) individuals were identified by the presence of only a 369-bp fragment, heterozygotes (AG) by the presence of both 231/138- and 369-bp fragments and homozygotes (GG) by the presence of only the 231- and 138-bp fragments. To rule out the incomplete digestion of the AG genotype, PCR products of this genotype were directly sequenced using the Applied Biosystems 310 automated DNA sequencer (Applied Biosystems, Foster City, CA, USA) following the manufacturer's instructions.

Site-directed mutagenesis and construction of CCR9-926A and 926G expression vectors

Site-directed mutagenesis of the human wild-type *CCR9* cDNA in pF1K vector (purchased from Kazusa DNA Research Institute, Kisarazu, Chiba, Japan) was carried out using the Quickchange Kit (Stratagene, La Jolla, CA, USA). Synthetic oligonucleotide primers containing the corresponding 926G point mutation had the following sequences: 5′-CCATTGACGCCTATGCCGTGTTCATC TCCAACTGT (forward) and 5′-ACAGTTGGAGA TGAACACGGCATAGGCGTCAATGG (reverse). The oligonucleotide was amplified with Pfu turbo DNA polymerase (Stratagene), and the template plasmid was digested by *Dpn*I. Each sequence of *CCR9* cDNA was amplified by PCR with primers containing the following *Eco*RI/*Not*I sites: 5′-CGCGGAATTCATGACACCCAC AGACTTCACA (forward) and 5′-ATCGGCGGCCGC TCAGAGGGAGAGTGCTCCTGAGGT (reverse). Each product was cut at *Eco*RI/*Not*I sites, and ligated into pMX-IRES-Puro (a kind gift from Dr Toshio Kitamura, University of Tokyo), which had been digested with *Eco*RI and *Not*I. The final construct used for cell transfection was sequenced entirely to verify the presence of the mutation and to ensure that no other variant was accidentally introduced during DNA amplification.

Retrovirus transfection

PLAT-A packaging cells (a kind gift from Dr Toshio Kitamura, University of Tokyo) were used to produce recombinant retrovirus particles.[11] PLAT-A cells were transfected with retroviral vectors using FuGENE6 (Roche, Indianapolis, MN, USA). Jurkat cells were infected with each of the pMX-CCR9-926A-IRES-Puro, pMX-CCR9-926G-IRES-Puro and pMX-IRES-Puro (control) retroviruses. The cells were washed once and resuspended in the fresh selection medium containing 500 ng/ml of puromycin (Cayla, Toulouse, France), 48 h after transfection .

Flow cytometric analysis

Phycoerythrin-labeled monoclonal anti-CCR9 (112509) was purchased from R&D Systems (Minneapolis, MN, USA). Analyses were carried out on FACSAria (BD Biosciences, San Jose, CA, USA) using the FlowJo software (Treestar, San Carlos, CA, USA).

Chemotaxis assays

Chemotaxis assays were carried out as previously described[12] using 6.5-mm-thick Transwell tissue culture inserts with a 5-μm pore size (Corning, Corning, NY, USA). The transfected cell lines were starved overnight in the plain RPMI 1640 medium, suspended at 1×10^7 cells per ml in this medium with 0.1% of BSA, and 100 μl of cell suspension was added to an upper insert in a lower well with 600 μl of the medium. After equilibration at 37 °C for 2 h, various concentrations (0–2000 ng/ml) of recombinant human CCL25 (R&D Systems) were added to the lower wells, and the plates were incubated for an additional 90 min before migrated cells in the lower well were counted.

Statistical analysis

OS was calculated from the date of transplantation to the date of death from any cause using the Kaplan–Meier method, and *P*-values were calculated using a log-rank test. Non-relapse mortality (NRM) was defined as mortality due to any cause other than relapse or disease progression. Cumulative incidences of NRM and relapse were estimated

using Gray's method, with relapse and NRM, respectively, as a competing risk. Acute GVHD was graded by established criteria.[13] Chronic GVHD was evaluated in patients who survived beyond day +100, and was classified as limited or extensive according to the Seattle criteria.[14] A multivariate Cox model was created for grade II–IV acute GVHD, organ stages of acute GVHD, chronic GVHD, OS, NRM and relapse using stepwise selection at a significance level of 5%. Age, conditioning, disease risk, remission state, donor–recipient sex combination and graft source were used as covariates. For chronic GVHD analysis, a history of acute GVHD was included as covariates. Hazard ratios of the *CCR9* genotype were adjusted by these models. In acute GVHD analysis, patients who died before day +30 were censored. Analysis was carried out using STATA (StataCorp. 2007; Stata Statistical Software: Release 10.0. Special Edition. Stata Corporation, College Station, TX, USA). Data analyses were completed as of January 2007 using the most updated database at each institute.

Results

Patient characteristics

Patient characteristics are summarized in Table 1. Ninety-four male patients and 73 female patients, with a median age of 38 years, were included in the study. Our patients were afflicted with various diseases, including myeloid malignancies ($n=106$), lymphoid malignancies ($n=42$) and benign diseases ($n=19$). Disease risk was standard in 97 patients and high in 70 patients. Standard risk included malignancies in the first and second remission, chronic myelogenous leukemia in the chronic phase, myelodysplastic syndrome with refractory anemia with or without ringed sideroblasts and benign diseases. High risk included all others. Ninety-eight patients with malignant disease received transplantation with their disease in remission. The graft source was BM in 130 patients and PBSCs in 37 patients. The conditioning regimen was myeloablative in 147 patients and reduced-intensity conditioning in 20 patients. TBI was used as part of the conditioning in 98 patients. Myeloablative conditioning regimens for malignancy included BU 16 mg/kg + CY 120 mg/kg ($n=32$), CY 120 mg/kg + TBI 12 Gy ($n=9$), CY 120 mg/kg + TBI 10 Gy + another agent of BU 8 mg/kg, cytarabine 8 g/m^2, etoposide 50 mg/kg or melphalan 140 mg/m^2 ($n=62$), BU 8 mg/kg + melphalan 180 mg/m^2 + TBI 10 Gy ($n=12$) and melphalan 180 mg/m^2 + TBI 10 Gy ($n=13$). Reduced-intensity conditioning regimens for malignancy included fludarabine 125 mg/m^2 + melphalan 100–180 mg/m^2 ($n=20$). Conditioning regimens for aplastic anemia included CY 200 mg/kg + TLI 7.5 Gy ($n=17$) and CY 200 mg/kg + TLI 5 Gy + TBI 5 Gy ($n=1$) as previously described.[15] One patient with paroxysmal nocturnal hemoglobinuria was conditioned with CY 120 mg/kg + TBI 12 Gy. At a median follow-up of 42 months (range: 2–220 months), 104 patients were still alive. The estimated 4-year OS, NRM and relapse rates were 55, 18 and 30%, respectively. Causes of 26 non-relapse mortalities included bronchiolitis obliterans ($n=2$), idiopathic pneumonia syndrome ($n=8$), hepatic failure ($n=1$), veno-occlusive

Table 1 Patient characteristics

No. of patients	167
Median age in years (range)	38 (15–62)
Sex (M/F)	94/73
Race (Japanese/other)	167/0
Disease	
AML	50
ALL	30
CML	40
MDS	16
ML	6
ATL	1
MM	5
AA	18
PNH	1
Disease risk	
Standard	97
High	70
Status at transplant among patients with malignant disease	
Remission	98
Non-remission	50
Graft source	
Bone marrow	130
PBSC	37
Gender compatibility	
Female donor in male recipient	45
Others	122
Conditioning	
TBI-containing conditioning	98
Myeloablative conditioning for malignancy	147
BU + CY	32
CY + TBI	9
CY + TBI + another agent	62
BU + melphalan + TBI	12
Melphalan + TBI	13
Reduced-intensity conditioning for malignancy	20
Fludarabine + melphalan	20
Conditioning for aplastic anemia/PNH	
CY + TLI	17
CY + TLI + TBI	1
CY + TBI	1
GVHD prophylaxis	
Cyclosporine + MTX	167
Overall survival at 4 years	55%
Non-relapse mortality at 4 years	18%
Relapse rate at 4 years	30%
Acute GVHD	
Grade (0/I/II/III/IV)	99/37/20/8/3
Skin stage (0/1/2/3/4)	104/33/6/22/2
Liver stage (0/1/2/3/4)	159/3/1/3/1
Gut stage (0/1/2/3/4)	153/4/2/5/3
Chronic GVHD (n = 155 evaluable)	
None	91
Limited/extensive	13/51
Organ (eye/oral/skin/lung/liver)	21/55/31/2/29

Abbreviations: AA = aplastic anemia; ATL = adult T-cell leukemia/lymphoma; F = female; M = male; MDS = myelodysplastic syndrome; ML = malignant lymphoma; MM = multiple myeloma; PNH = paroxysmal nocturnal hemoglobinuria.

Table 2 Proportion of patients who developed GVHD in each genotype

Events	*Genotype 926AG*	*Genotype 926AA*
Acute GVHD		
Grade II–IV	2/10 (20%)	29/157 (18%)
Skin stage 2–4	4/10 (40%)	26/157 (17%)
Liver stage 2–4	1/10 (10%)	4/157 (2.5%)
Gut stage 2–4	1/10 (10%)	9/157 (5.7%)
Chronic GVHD		
Limited/extensive	4/10 (40%)	60/145 (41%)
Eye	2/10 (20%)	19/145 (13%)
Oral	4/10 (40%)	51/145 (35%)
Skin	3/10 (30%)	28/145 (19%)
Lung	1/10 (10%)	1/145 (0.6%)
Liver	2/10 (20%)	27/145 (19%)

disease ($n=2$), hepatitis ($n=2$), intestinal bleeding ($n=1$), transplant-associated microangiopathy ($n=3$), acute GVHD ($n=3$), scleroderma ($n=1$) and bacterial or fungal pneumonia ($n=3$). The incidence rates of grade II–IV, III–IV acute GVHD and chronic limited/extensive GVHD were 18.6, 6.6 and 41%, respectively. The incidence rates of stage 2–4 skin, liver and gut involvement were 18, 3 and 6%, respectively.

Frequency of CCR9 genotypes

Ten donors had genotype 926AG by the RFLP method, which was subsequently confirmed using direct sequence. The frequencies of the 926AA, 926AG and 926GG genotypes among the donors were 94, 6 and 0%, respectively, which were comparable with those reported in the HapMap-JPT database (http://www.hapmap.org).

Hazard analysis and the effect of CCR9 genotypes on transplant outcome

The proportion of patients who developed GVHD in each genotype is summarized in Table 2. Grade II–IV GVHD, stage 2–4 skin GVHD, stage 2–4 liver GVHD, stage 2–4 gut GVHD and chronic limited/extensive GVHD developed in 2, 4, 1, 1 and 4 patients, respectively, among patients whose donor had the genotype 926AG, whereas they developed in 29, 26, 4, 9 and 60 patients, respectively, among patients whose donor had the genotype 926AA. The estimated 4-year OS, NRM and relapse rates were not significantly different between G926A genotypes (56 vs 55%, $P=0.78$; 33 vs 17%, $P=0.32$; 10 vs 32%, $P=0.19$, respectively) (Figure 1). Multivariate analyses showed that PBSC transplantation was a risk factor for grade II–IV GVHD, stage 2–4 skin GVHD and stage 2–4 gut GVHD; high risk disease was a risk factor for OS and relapse; age of more than 40 years was a risk factor for OS and NRM; and female-to-male transplantation was a risk factor for chronic liver GVHD (Table 3, middle column). Hazard ratios of the genotype 926AG, adjusted by these factors, are listed in Table 3 (right column). The genotype 926AG was significantly associated with acute stage 2–4 skin GVHD (hazard ratio: 3.2; 95% confidence interval (95% CI): 1.1–9.1; $P=0.032$) and chronic skin GVHD (hazard ratio: 4.1; 95% CI: 1.1–15; $P=0.036$), whereas it was not

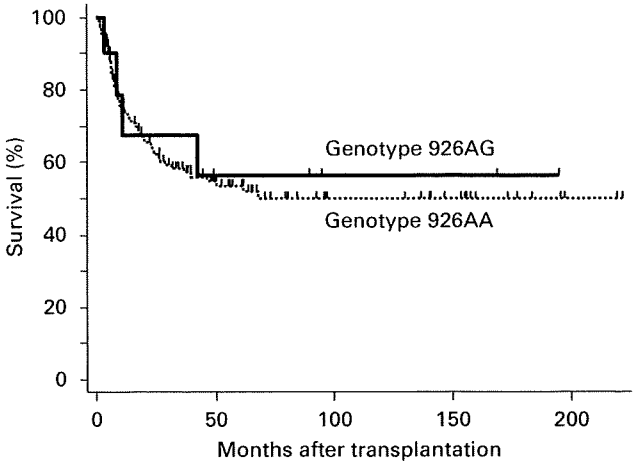

Figure 1 Overall survival between G926A genotypes. At a median follow-up of 42 months (range: 2–220 months), the estimated 4-year overall survival was not statistically different between G926A genotypes (56 vs 55%, $P=0.78$).

associated with grade II–IV GVHD or with stage 2–4 liver GVHD, stage 2–4 gut GVHD, limited or extensive chronic GVHD, chronic GVHD in organs other than skin, OS, NRM or relapse. PBSCs were used in only 1 of 10 patients who received transplantation from 926AG donors.

Functional comparison between CCR9-926A and 926G

To clarify the functional differences between genotypes of 926A and 926G, we created cDNA constructs with each genotype using the Quickchange Kit. Each construct was transfected into Jurkat cells with retroviral vectors. After 3 weeks of selection with puromycin, we analyzed the expression of CCR9 in each of the stably transfected cells. Cells were stained with phycoerythrin-labeled monoclonal anti-CCR9. The level of CCR9 expression was higher in CCR9-transfected cells compared with that in control-transfected cells, and equivalent between the 926A and 926G genotypes (Figure 2a).

We next analyzed the migration of Jurkat cells transfected with control vectors, 926A and 926G, as well as plain Jurkat cells in response to varying concentrations of CCL25, using porous Transwell tissue culture inserts to separate the cells in the upper chambers from the chemokine-containing medium in the lower chambers. As shown in Figure 2b, *CCR9*-transfected cells, but not the control-transfected or plain Jurkat cells, migrated in response to CCL25 in a dose-dependent manner, producing a bell-shaped curve. It is noted that *CCR9*-926G-expressing cells were more responsive to CCL25 compared with those expressing *CCR9*-926A.

Discussion

Several genetic polymorphisms of inflammatory cytokine genes are reported to affect the outcome of allo-HSCT.[16–21] Chemokines are another group of cytokines that control the trafficking of leukocytes through interactions with chemokine receptors. We hope to clarify the role of these

Table 3 Effect of the *CCR9* genotype on transplant outcome

Events	*Risk factor(s)*	*Multivariate*[a]		*Genotype 926AG*[b]	
		Hazard ratio (CI)	P-*value*	*Hazard ratio (CI)*	P-*value*
Acute GVHD					
Grade II–IV	PBSCT	3.4 (1.7–6.9)	0.001	1.2 (0.30–5.3)	0.76
Skin stage 2–4	PBSCT	2.7 (1.3–5.5)	0.008	3.2 (1.1–9.1)	0.032
Liver stage 2–4	—	—	—	4.2 (0.47–37)	0.20
Gut stage 2–4	PBSCT	5.7 (1.6–20)	0.007	2.4 (0.30–19)	0.41
Chronic GVHD					
Limited/extensive	—	—	—	1.7 (0.52–5.8)	0.37
Eye	—	—	—	6.2 (0.56–68)	0.14
Oral	—	—	—	2.4 (0.71–8.4)	0.16
Skin	—	—	—	4.1 (1.1–15)	0.036
Lung	—	—	—	12 (0.76–196)	0.077
Liver	Female to male	3.5 (1.0–12)	0.05	1.7 (0.21–13)	0.63
Overall survival	Age > 40	2.1 (1.3–3.6)	0.004	0.84 (0.30–2.3)	0.73
	High risk	2.1 (1.3–3.6)	0.004		
Non-relapse mortality	Age > 40	2.7 (1.2–6.1)	0.015	1.3 (0.40–4.5)	0.64
Relapse	High risk	4.0 (2.0–7.8)	<0.001	0.36 (0.05–2.6)	0.31

Abbreviations: CI = confidence interval; PBSCT = peripheral blood stem cell transplantation.
[a]Covariates used were age, conditioning, disease risk, remission state, donor–recipient sex combination and graft source. For chronic GVHD analysis, history of acute GVHD was included in the covariates. Only significant factors were listed.
[b]Adjusted by significant factors.

chemokines in initiating GVHD. Specifically, we address the association of polymorphism in the tissue-specific chemokine receptor gene with acute and chronic GVHD and the regulation of leukocyte trafficking.

CCL25 and CCR9 (as chemokine and chemokine receptor) are selectively expressed in both the thymus and the small intestine.[22,23] One of their important functions is the selective homing and retention of CCR9-positive T cells and B cells to the small intestine rather than to the colon, which provides a mechanism for regional specialization of the mucosal immune system.[9,24] Another function is regulating intrathymic T-cell development, particularly double-negative to double-positive transition,[25,26] which may be associated with T-cell recovery after allo-HSCT. Therefore, the effect of the *CCR9* genotype on acute GVHD is hypothesized to result from its function in the small intestine because T cells educated in the thymus will appear at least 6 months after transplantation.[27]

Interestingly, donor *CCR9* SNPs affected the incidence of skin GVHD, but did not affect the incidence of intestinal GVHD. This observation may be partially explained by the findings of Beilhack *et al.*,[28] who recently reported the redundancy of secondary lymphoid organs at different anatomical sites in GVHD initiation. They suggested that primed T cells could initiate GVHD at sites other than their original priming sites. As Peyer's patches are important sites of Ag presentation,[29] differences in T cell homing to Peyer's patches between each *CCR9* genotype may produce changes in Ag presentation and result in varying incidences of skin GVHD.

Our results suggest the possibility of CCL25/CCR9-targeting modalities for GVHD. CCL25 and CCR9 have an important role in the adherence of T lymphocytes to the intestinal endothelium under inflammatory and normal conditions, and anti-CCL25 Ab attenuates the TNF-α-induced T-cell adhesion in the small intestine.[30] Although blocking the interactions of CCL25 and CCR9 may delay immunological reconstitution in the thymus, CCR9-deficient mice showed no major effect on intrathymic T-cell development despite a 1-day lag in the appearance of double-positive cells and a diminution of γδ-T cells.[31]

One possible limitation of this study is that genetic associations can be biased by population stratification,[32] and there is also the chance of false-positive associations with the *CCR9* genotype on the basis of multiple statistical tests. Confirmation of the results with another separate cohort is needed for eliminating a possible confounding effect. Another limitation is that this SNP might be in linkage disequilibrium with SNPs in the *CCR9* gene or in the other genes located nearby. Linkage disequilibrium mapping of *CCR9* using the HapMap-JPT database showed one small block in introns of the *CCR9* gene, but G926A was outside the block with no known associations with other SNPs in the *CCR9* gene or with genes located around chromosome 3p21.3. In addition, this SNP alters CCR9 amino acid sequences of the third exoloop, which is an important site for chemokine binding and specificity.[33] Therefore, this SNP can affect biological functions due to altered efficiencies of the receptor or signal transduction from the receptor. Although Transwell assays using SNP-transfected cells showed that biological functions varied according to this SNP, the elucidation of additional mechanisms are matters for future research.

In summary, this study suggests that donor 926AG is associated with an increased incidence of acute and chronic skin GVHD in related HSCT recipients. CCL25 and CCR9

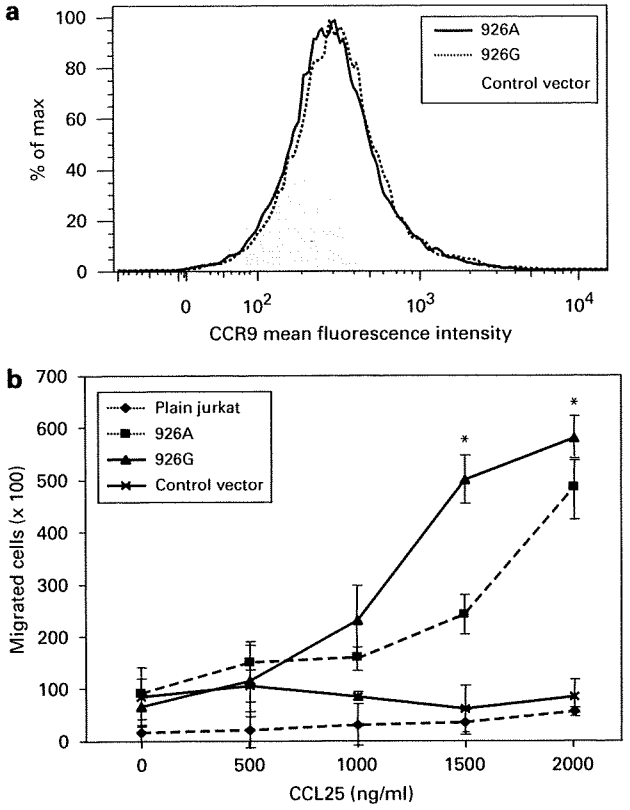

Figure 2 Chemotaxis assays with *CCR9*-polymorphism-transfected Jurkat cells: (**a**) Flow cytometric analysis of CCR9 expression. Transfected Jurkat cells were stained with phycoerythrin (PE)-labeled monoclonal anti-CCR9. Control staining with control-transfected Jurkat cells is also shown (shadow); (**b**) Jurkat cells transfected with cDNAs encoding *CCR9* migrated in response to CCL25. After puromycin selection, 1×10^6 transfected cells and the same number of Jurkat cells were added to porous Transwell tissue culture inserts and placed in wells containing various concentrations of CCL25. After 90-min of incubation, cells migrating through the membranes into the lower wells were counted. Results are expressed as cells migrating per 10^6 input cells. Assays were carried out in triplicate and error bars represent s.d. $^*P<0.05$

may be candidates for future therapeutic targets that alter the quality and incidence of GVHD.

Conflict of interest

The authors declare no conflict of interest.

Acknowledgements

We thank Dr Toshio Kitamura for providing the pMX-IRES-Puro vector and PLAT-A packaging cells. This study was supported in part by a Health and Labor Science Research Grant (20251001) from the Ministry of Health, Labour and Welfare of Japan, a Grant-in-Aid for Scientific Research (20591149 and 19591105) from the Ministry of Education, Culture, Sports, Science and Technology, and Grants-in-Aid from the National Institute of Biomedical Innovation and the Sankyo Memorial Foundation, Japan.

References

1 Perfetti P, Carlier P, Strada P, Gualandi F, Occhini D, Van Lint MT *et al.* Extracorporeal photopheresis for the treatment of steroid refractory acute GVHD. *Bone Marrow Transplant* 2008; **42**: 609–617.
2 Kunkel EJ, Butcher EC. Chemokines and the tissue-specific migration of lymphocytes. *Immunity* 2002; **16**: 1–4.
3 Campbell DJ, Kim CH, Butcher EC. Chemokines in the systemic organization of immunity. *Immunol Rev* 2003; **195**: 58–71.
4 Campbell JJ, Butcher EC. Chemokines in tissue-specific and microenvironment-specific lymphocyte homing. *Curr Opin Immunol* 2000; **12**: 336–341.
5 Moser B, Loetscher P. Lymphocyte traffic control by chemokines. *Nat Immunol* 2001; **2**: 123–128.
6 Pan J, Kunkel EJ, Gosslar U, Lazarus N, Langdon P, Broadwell K *et al.* A novel chemokine ligand for CCR10 and CCR3 expressed by epithelial cells in mucosal tissues. *J Immunol* 2000; **165**: 2943–2949.
7 Wang W, Soto H, Oldham ER, Buchanan ME, Homey B, Catron D *et al.* Identification of a novel chemokine (CCL28), which binds CCR10 (GPR2). *J Biol Chem* 2000; **275**: 22313–22323.
8 Kunkel EJ, Campbell JJ, Haraldsen G, Pan J, Boisvert J, Roberts AI *et al.* Lymphocyte CC chemokine receptor 9 and epithelial thymus-expressed chemokine (TECK) expression distinguish the small intestinal immune compartment: epithelial expression of tissue-specific chemokines as an organizing principle in regional immunity. *J Exp Med* 2000; **192**: 761–768.
9 Papadakis KA, Prehn J, Nelson V, Cheng L, Binder SW, Ponath PD *et al.* The role of thymus-expressed chemokine and its receptor CCR9 on lymphocytes in the regional specialization of the mucosal immune system. *J Immunol* 2000; **165**: 5069–5076.
10 Stenstad H, Svensson M, Cucak H, Kotarsky K, Agace WW. Differential homing mechanisms regulate regionalized effector CD8alphabeta+ T cell accumulation within the small intestine. *Proc Natl Acad Sci U S A* 2007; **104**: 10122–10127.
11 Onishi M, Kinoshita S, Morikawa Y, Shibuya A, Phillips J, Lanier LL *et al.* Applications of retrovirus-mediated expression cloning. *Exp Hematol* 1996; **24**: 324–329.
12 Yu CR, Peden KW, Zaitseva MB, Golding H, Farber JM. CCR9A and CCR9B: two receptors for the chemokine CCL25/TECK/Ck beta-15 that differ in their sensitivities to ligand. *J Immunol* 2000; **164**: 1293–1305.
13 Przepiorka D, Weisdorf D, Martin P, Klingemann HG, Beatty P, Hows J *et al.* 1994 Consensus Conference on Acute GVHD Grading. *Bone Marrow Transplant* 1995; **15**: 825–828.
14 Sullivan KM, Agura E, Anasetti C, Appelbaum F, Badger C, Bearman S *et al.* Chronic graft-versus-host disease and other late complications of bone marrow transplantation. *Semin Hematol* 1991; **28**: 250–259.
15 Inamoto Y, Suzuki R, Kuwatsuka Y, Yasuda T, Takahashi T, Tsujimura A *et al.* Long-term outcome after bone marrow transplantation for aplastic anemia using cyclophosphamide and total lymphoid irradiation as conditioning regimen. *Biol Blood Marrow Transplant* 2008; **14**: 43–49.
16 Kallianpur AR. Genomic screening and complications of hematopoietic stem cell transplantation: has the time come? *Bone Marrow Transplant* 2005; **35**: 1–16.
17 Dickinson AM, Middleton PG, Rocha V, Gluckman E, Holler E. Genetic polymorphisms predicting the outcome of bone marrow transplants. *Br J Haematol* 2004; **127**: 479–490.
18 Lin MT, Storer B, Martin PJ, Tseng LH, Gooley T, Chen PJ *et al.* Relation of an interleukin-10 promoter polymorphism to graft-versus-host disease and survival after hematopoietic-cell transplantation. *N Engl J Med* 2003; **349**: 2201–2210.

19 Socie G, Loiseau P, Tamouza R, Janin A, Busson M, Gluckman E *et al.* Both genetic and clinical factors predict the development of graft-versus-host disease after allogeneic hematopoietic stem cell transplantation. *Transplantation* 2001; **72**: 699–706.
20 Cavet J, Dickinson AM, Norden J, Taylor PR, Jackson GH, Middleton PG. Interferon-gamma and interleukin-6 gene polymorphisms associate with graft-versus-host disease in HLA-matched sibling bone marrow transplantation. *Blood* 2001; **98**: 1594–1600.
21 Mehta PA, Eapen M, Klein JP, Gandham S, Elliott J, Zamzow T *et al.* Interleukin-1 alpha genotype and outcome of unrelated donor haematopoietic stem cell transplantation for chronic myeloid leukaemia. *Br J Haematol* 2007; **137**: 152–157.
22 Zaballos A, Gutierrez J, Varona R, Ardavin C, Marquez G. Cutting edge: identification of the orphan chemokine receptor GPR-9-6 as CCR9, the receptor for the chemokine TECK. *J Immunol* 1999; **162**: 5671–5675.
23 Zabel BA, Agace WW, Campbell JJ, Heath HM, Parent D, Roberts AI *et al.* Human G protein-coupled receptor GPR-9-6/CC chemokine receptor 9 is selectively expressed on intestinal homing T lymphocytes, mucosal lymphocytes, and thymocytes and is required for thymus-expressed chemokine-mediated chemotaxis. *J Exp Med* 1999; **190**: 1241–1256.
24 Mora JR, von Andrian UH. Role of retinoic acid in the imprinting of gut-homing IgA-secreting cells. *Semin Immunol* 2009; **21**: 28–35.
25 Wurbel MA, Philippe JM, Nguyen C, Victorero G, Freeman T, Wooding P *et al.* The chemokine TECK is expressed by thymic and intestinal epithelial cells and attracts double- and single-positive thymocytes expressing the TECK receptor CCR9. *Eur J Immunol* 2000; **30**: 262–271.
26 Norment AM, Bogatzki LY, Gantner BN, Bevan MJ. Murine CCR9, a chemokine receptor for thymus-expressed chemokine that is up-regulated following pre-TCR signaling. *J Immunol* 2000; **164**: 639–648.
27 Heitger A, Neu N, Kern H, Panzer-Grumayer ER, Greinix H, Nachbaur D *et al.* Essential role of the thymus to reconstitute naive (CD45RA+) T-helper cells after human allogeneic bone marrow transplantation. *Blood* 1997; **90**: 850–857.
28 Beilhack A, Schulz S, Baker J, Beilhack GF, Nishimura R, Baker EM *et al.* Prevention of acute graft-versus-host disease by blocking T-cell entry to secondary lymphoid organs. *Blood* 2008; **111**: 2919–2928.
29 Niess JH, Reinecker HC. Lamina propria dendritic cells in the physiology and pathology of the gastrointestinal tract. *Curr Opin Gastroenterol* 2005; **21**: 687–691.
30 Hosoe N, Miura S, Watanabe C, Tsuzuki Y, Hokari R, Oyama T *et al.* Demonstration of functional role of TECK/CCL25 in T lymphocyte-endothelium interaction in inflamed and uninflamed intestinal mucosa. *Am J Physiol Gastrointest Liver Physiol* 2004; **286**: G458–G466.
31 Wurbel MA, Malissen M, Guy-Grand D, Meffre E, Nussenzweig MC, Richelme M *et al.* Mice lacking the CCR9 CC-chemokine receptor show a mild impairment of early T- and B-cell development and a reduction in T-cell receptor gammadelta(+) gut intraepithelial lymphocytes. *Blood* 2001; **98**: 2626–2632.
32 Wacholder S, Rothman N, Caporaso N. Counterpoint: bias from population stratification is not a major threat to the validity of conclusions from epidemiological studies of common polymorphisms and cancer. *Cancer Epidemiol Biomarkers Prev* 2002; **11**: 513–520.
33 Youn BS, Yu KY, Oh J, Lee J, Lee TH, Broxmeyer HE. Role of the CC chemokine receptor 9/TECK interaction in apoptosis. *Apoptosis* 2002; **7**: 271–276.

Biochemical and Biophysical Research Communications 390 (2009) 48–53

Contents lists available at ScienceDirect

Biochemical and Biophysical Research Communications

journal homepage: www.elsevier.com/locate/ybbrc

Escape mechanisms from antibody therapy to lymphoma cells: Downregulation of *CD20* mRNA by recruitment of the HDAC complex and not by DNA methylation

Takumi Sugimoto [a], Akihiro Tomita [a,*], Junji Hiraga [a,b], Kazuyuki Shimada [a], Hitoshi Kiyoi [c], Tomohiro Kinoshita [a], Tomoki Naoe [a]

[a] *Department of Hematology and Oncology, Nagoya University Graduate School of Medicine, Nagoya, Japan*
[b] *Department of Hematology, Toyota Memorial Hospital, Toyota, Japan*
[c] *Department of Infectious Diseases, Nagoya University School of Medicine, Nagoya, Japan*

ARTICLE INFO

Article history:
Received 15 September 2009
Available online 19 September 2009

Keywords:
CD20
Rituximab
Epigenetics
Histone deacetylases
DNA methytransferases

ABSTRACT

Although rituximab is a critical monoclonal antibody therapy for CD20-positive B-cell lymphomas, rituximab resistance showing a CD20-negative phenotypic change has been a considerable clinical problem. Here we demonstrate that *CD20* mRNA and protein expression is repressed by recruitment of a histone deacetylase protein complex to the *MS4A1* (*CD20*) gene promoter in CD20-negative transformed cells after treatment with rituximab. *CD20* mRNA and protein expression were stimulated by decitabine (5-Aza-dC) in CD20-negative transformed cells, and was enhanced by trichostation A (TSA). Immunoblotting indicated that DNMT1 expression was first downregulated 1 day after treatment with 5-Aza-dC, but IRF4 and Pu.1, the transcriptional regulators of *MS4A1*, were still expressed with or without 5-Aza-dC. Interestingly, CpG methylation of the *MS4A1* promoter was not observed in CD20-negative transformed cells without 5-Aza-dC. A chromatin immunoprecipitation (ChIP) assay indicated that the Sin3A–HDAC1 co-repressor complex was recruited to the promoter and dissociated from the promoter with 5-Aza-dC and TSA, resulting in histone acetylation. Under these conditions, IRF4 and Pu.1 were continually recruited to the promoter with or without 5-Aza-dC and TSA. These results suggest that recruitment of the Sin3A–HDAC1 complex is related to downregulation of CD20 expression in CD20-negative B-cells after treatment with rituximab.

Introduction

Rituximab is the first therapeutic monoclonal antibody targeting human malignant tumors, and is now an indispensable molecular-targeting drug for CD20-positive B-cell lymphomas [1–3]. Although the effectiveness is significant, resistance to rituximab has also become a considerable problem [4].

Several mechanisms of the resistance have been suggested, including loss of CD20 protein expression after rituximab use [5–12] and CD20 gene mutations [13]. Furthermore, other mechanisms have also been suggested [4] such as internalization of CD20 protein [14], interference with accessibility of rituximab to CD20 protein by inhibitory factors, rapid metabolism of the antibody, abnormalities in B-cell signaling in tumor cells [15], abnormalities of apoptosis [16], antibody-dependent cell-mediated cytotoxicity (ADCC), and complement-dependent cytotoxicity (CDC) [17].

Very recently, we reported observation of downregulation of CD20 protein expression in CD20-positive B-cell lymphoma patients after treatment with rituximab-containing combination chemotherapies [6,7]. In those cases, it was strongly suggested that aberrant downregulation of *MS4A1* expression was closely related to the loss of CD20 protein expression, and that expression of CD20 and rituximab sensitivity were partially restored by some molecular-targeting drugs [6,7]. Although these findings suggest that epigenetic mechanisms, in part, contribute to the downregulation of CD20 expression, the molecular mechanisms are still not clear. Furthermore, a recent report indicated that reduced CD20 protein expression in *de novo* diffuse large B-cell lymphoma is associated with a poor survival rate [18]. Thus, understanding the mechanisms of downmodulation of CD20 protein expression is likely to be very important from both basic research and clinical viewpoints.

In this report, we show that the recruitment of a histone deacetylase (HDAC) co-repressor complex to the *MS4A1* promoter

* Corresponding author. Address: Department of Hematology and Oncology, Nagoya University Graduate School of Medicine, Tsurumai-Cho 65, Showa-ku, Nagoya 466-8560, Japan. Fax: +81 52 744 2161.
E-mail address: atomita@med.nagoya-u.ac.jp (A. Tomita).

0006-291X/$ - see front matter © 2009 Elsevier Inc. All rights reserved.
doi:10.1016/j.bbrc.2009.09.059

region, but not DNA methylation [19], is involved in CD20-negative phenotypic changes in B-cell lymphoma cells after treatment with rituximab. We show that the complex dissociated from the promoter in the presence of a DNA methyltransferase (DNMT) inhibitor and a HDAC inhibitor [20], resulting in partial restoration of CD20 expression.

Materials and methods

Cell culture conditions and treatment with epigenetic drugs. RRBL1 [6], Raji, and NALM6 cells were cultured in RPMI 1640 medium (Sigma–Aldrich, St. Louis, MO, USA) with 10% fetal calf serum. Five-Aza-dC (5-aza-2′-deoxycytidine; Sigma, St. Louis, MO) and TSA (Sigma) at final concentrations of 100 μM and 100 nM, respectively, were added directly to the culture medium.

Immunoblotting. Cells (~5×10^5) were lysed in 100 μl of lysis buffer (50 mM Tris–HCl, pH 8.0, 1.5 mM $MgCl_2$, 1 mM EGTA, 5 mM KCl, 10% glycerol, 0.5% NP-40, 300 mM NaCl, 0.2 mM PMSF, 1 mM DTT, and a complete mini protease inhibitor tablet (Roche)). After centrifugation at 10,000 *g* for 10 min, the supernatants were placed in new tubes, and 100 μl of 2× SDS sample buffer was added. After boiling for 5 min, samples were separated with SDS–polyacrylamide gel electrophoresis (SDS–PAGE). Immunoblotting was carried out as described previously [21,22] using anti-CD20, -IRF4, -Pu.1, -GAPDH antibodies (Santa Cruz Biotechnology, Santa Cruz, CA, USA), and anti-DNMT1 antibody (Abcam, Cambridge, MA, USA).

RNA preparation and reverse transcriptase-polymerase chain reaction (RT-PCR). RNA from cell lines (1×10^5 cells) was obtained using Trizol (Invitrogen, Carlsbad, CA, USA). Complementary DNA (cDNA) was prepared as reported previously [7,22].

For RT-PCR, the following primers were designed: CD20-U; 5′-ATGAAAGGCCCTATTGCTATG-3′, CD20-L; 5′-GCTGGTTCACAGTTGTATATG-3′, β-actin-U; 5′-TCACTCATGAAGATCCTCA-3′, and β-actin-L; 5′-TTCGTGGATGCCACAGGAC-3′. Semi-quantitative RT-PCR with AmpliTaq Gold was performed as described previously [6].

Methylation status of the MS4A1 promoter. To examine the methylation status, bisulfite sequencing was performed. Genomic DNA was prepared with a QIAamp DNA Blood Mini kit (Qiagen, Valencia, CA, USA). Bisulfite treatment was performed using EpiTect Bisulfite kits (Qiagen). After bisulfite treatment, PCR of the *MS4A1* promoter was performed using the specific primers as follows, MS4A1-pro-MSPU; 5′-GGTAGTATGAGTATGTTAGGTAGTT-3′, MS4A1-pro-MSPL; 5′-TTTTCCTTACCTAAATCTCCAAAA-3′. PCR fragments were cloned into a pGEM-T easy vector (Promega, Madison, WI, USA) and sequenced.

Flow cytometry (FCM) analysis. Cell surface antigens of RRBL1 with or without 5-Aza-dC and TSA treatment were analyzed using a BD FACSCalibur Flow Cytometer (BD Bioscience, Franklin Lakes, NJ, USA) with anti-CD20 antibody (Leu-16 PE, BD) and mouse IgG1 κ isotype control (PE-Cy7, BD).

Chromatin immunoprecipitation (ChIP) assay. The ChIP assay was performed as described previously [22,23]. For immunoprecipitation (IP), the following antibodies were used; anti-Pu.1, -IRF4 (Santa Cruz Biotechnology), -acetylated H4 (Millipore, Billerica, MA, USA), -Sin3A, and anti-HDAC1 (Abcam) antibodies. Immunoprecipitated DNA was used for semi-quantitative PCR using LA-Taq polymerase (TAKARA, Ohtsu, Japan). The following primers for the *MS4A1* promoter and 3′-intron sequence (negative control) were used; CD20pro-U; 5′-CTAAAAGTGAAGCCAGAAGG-3′, CD20pro-L; 5′-GGAGGGTGAGTGGTGTAGT-3′, CD20-3′U; 5′-GCTGACCTCACATAACTCCT-3′, CD20-3′L; 5′-GAAATCCCTCAGACTCAGAC-3′.

Immunoprecipitation (IP) assay. The IP assay was carried out as described previously [22]. Whole cell lysate was obtained from RRBL1 cells (1×10^7) using 800 μl of lysis buffer. After adding 800 μl of lysis buffer without NP-40 and NaCl, the lysate was divided into four tubes (400 μl each) and IP using anti-IRF4, -Sin3A, and -HDAC1 antibodies was performed. The precipitated samples were applied to SDS–PAGE followed by immunoblotting. For the pre-IP samples, 5% of the whole cell lysate was used.

Results

CD20 protein and mRNA expression were stimulated by treatment with 5-Aza-dC in CD20-negative transformed cells

As we reported previously [6,7], the downregulation of CD20 protein and mRNA expression has been observed in some CD20-positive B-cell lymphoma patients after treatment with rituximab-containing chemotherapies. We also reported that the downregulation of CD20 expression was partially stimulated by treatment with the epigenetic drugs 5-Aza-dC and TSA. RRBL1 cells were established from a patient with B-cell lymphoma who showed a CD20-negative phenotypic change after treatment with rituximab [6]. To examine the mechanisms of stimulation of CD20 expression by 5-Aza-dC, we examined the protein expression pattern that may affect CD20 gene transcription in RRBL1 cells. RRBL1 cells were treated with 5-Aza-dC for 24 h, and were then washed and incubated for up to 7 days (Fig. 1A). During this procedure, the cells were harvested several times as indicated and analyzed using semi-quantitative RT-PCR and immunoblotting (IB) (Fig. 1B). *CD20* mRNA and protein expression were stimulated by 5-Aza-dC, and the peak of expression was observed around day 3 after treatment with 5-Aza-dC (lane 6). After day 5, CD20 protein expression had gradually decreased. DNMT1 depletion was confirmed at 24 h after treatment with 5-Aza-dC (lane 4) as reported previously [24]. IRF4 and Pu.1 are transcription factors that interact with the *MS4A1* promoter and regulate CD20 expression [25]. IRF4/Pu.1 was almost constantly expressed throughout the 5-Aza-dC treatment duration (lanes 3–8), but only a modest upregulation was observed after treatment with 5-Aza-dC around day 2 (lane 5). These results suggested that DNMT1 depletion by 5-Aza-dC may be related to stimulation of *MS4A1* expression.

DNA methylation status of the MS4A1 promoter

To explain the activation of *CD20* mRNA and protein expression after treatment with 5-Aza-dC in RRBL1 cells, we next examined the CpG methylation status of the *MS4A1* promoter (Fig. 1C). Interestingly, CpG islands were not observed on the promoter region located ~5 kb upstream from the transcription start site, and only four CG sites were found on the promoter from the −1000 to +100 region. Bisulfite sequencing was carried out to confirm methylated CpG. As shown in Fig. 1C, no CpG methylation was observed on the three CpG sites around the transcription start site in RRBL1 cells. In NALM6 cells, a CD20-negative lymphoblastic leukemia cell line, several methylated CpGs were observed. Furthermore, the same analysis was performed using primary tumor cells from a patient suffering from CD20-negative transformed B-cell lymphoma after treatment with rituximab-containing combination chemotherapies. (Detailed information about this patient is described in our previous paper as UPN3 [7]). The three CpG sites were not methylated, as observed in RRBL1 cells (Fig. 1C, UPN3). These results suggest that transcriptional activation of *MS4A1* by 5-Aza-dC may not be regulated by its promoter CpG demethylation in RRBL1 cells.

Histone deacetylase inhibitor TSA enhances CD20 expression by 5-Aza-dC in CD20-negative transformed cells

Next, we analyzed the effect of a HDAC inhibitor in addition to 5-Aza-dC on *MS4A1* expression in RRBL1 cells. CD20 protein expression in RRBL1 cells was confirmed using immunoblotting

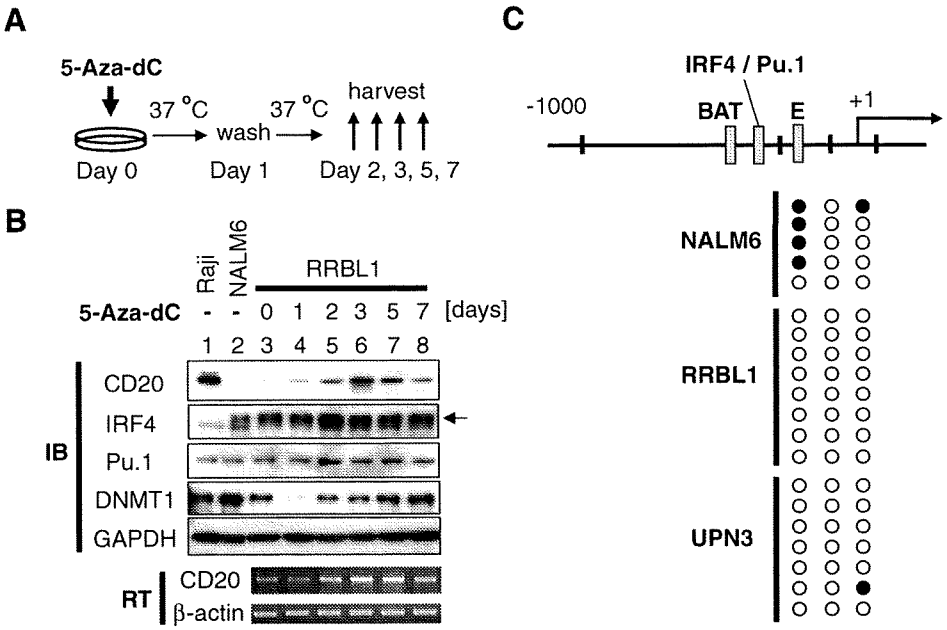

Fig. 1. CD20 protein and mRNA expression were transiently stimulated by treatment with a DNMT inhibitor. (A) Schematic representation of 5-Aza-dC treatment of the CD20-negative transformed B-lymphoma cells. RRBL1 cells were incubated at 37 °C for 24 h, and then washed twice with RPMI medium with 10% FCS without 5-Aza-dC. Cells were further incubated for up to 7 days, and were harvested at days 1, 2, 3, 5, and 7. (B) Protein expression was examined using immunoblotting (IB) with the indicated antibodies. The mRNA expression level was determined using semi-quantitative RT-PCR (RT). The black arrow indicates the band for IRF4. Raji and NALM6 cells were used as positive and negative controls, respectively. GAPDH and β-actin were measured as internal controls. (C) The structure of the *MS4A1* promoter near the transcription start site (from −1000 to +100) is depicted. The BAT-box, IRF4/Pu.1 binding sites, and E-box are shown as shaded boxes. Only four CpG sites, which are putative methylation sites, were found and are shown as black vertical bars. The methylation status of the three CpG sites around the transcription start site in NALM6, RRBL1, and primary B-lymphoma cells that show CD20-negative transformation was analyzed with bisulfite sequencing. Five to eight clones were analyzed from each sample. Black and open circles indicate methylated and non-methylated CpGs, respectively.

and flow cytometry (FCM) (Fig. 2A and B) following treatment with 5-Aza-dC and/or TSA. When RRBL1 cells were treated with 5-Aza-dC or TSA alone, minimal activation of CD20 protein expression was observed using immunoblotting (Fig. 2A, lanes 4 and 5) and FCM (Fig. 2B, 5-Aza-dC). In the presence of 5-Aza-dC and TSA, CD20 protein expression was significantly increased (Fig. 2A, lane 6, and B, 5-Aza-dC + TSA). These results suggested that *MS4A1* expression is, in part, regulated by epigenetic mechanisms such as histone modification including lysine acetylation, rather than DNA CpG methylation of the *MS4A1* promoter.

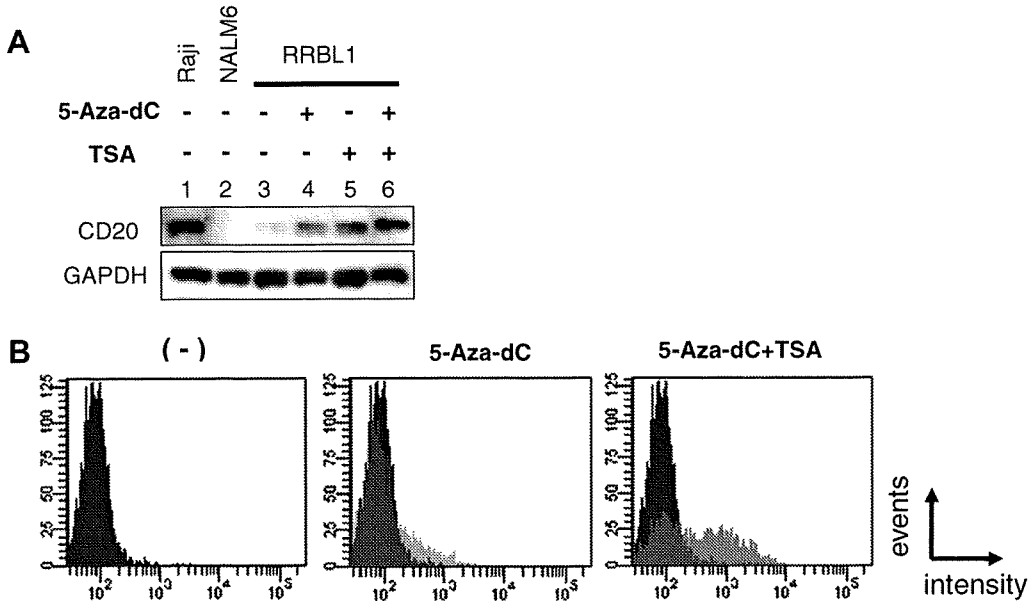

Fig. 2. CD20 protein expression by 5-Aza-dC was enhanced by TSA. CD20 protein expression was shown with IB (A) and FCM (B) with or without epigenetic drugs. For 5-Aza-dC treatment, RRBL1 cells were incubated with 5-Aza-dC for 24 h followed by washing and two additional days of incubation. TSA was added at the start of day 3, and cells were incubated for 24 h. If cells were not treated with 5-Aza-dC, washing was also carried out at day 1 to adjust the incubation conditions. All the cells were harvested at day 4 and utilized for IB and FCM analyses. The untreated and treated cells with the epigenetic drugs were depicted as black and gray areas, respectively (B).